



**EXPERIMENTAL AND NUMERICAL STUDY TO INCREASE THE  
EFFICIENCY OF THE PHOTOVOLTIC THERMAL SYSTEM USING PCM**

**THESIS**

**SUBMITTED TO THE DEPARTMENT OF MECHANICAL ENGINEERING  
TECHNIQUES OF POWER**

**IN PARTIAL FULFILLMENT OF THE REQUIREMENTS FOR THE  
DEGREE OF MASTER THERMAL TECHNOLOGIES IN MECHANICAL  
ENGINEERING TECHNIQUES OF POWER (M.TECH.)**

**BY**

**AMMAR MAYTHEM FAISEL**

Supervised by  
Dr. Ali Najah Kadhim

Aug/2022

## DECLARATION

I confirm that the work in this thesis is entirely mine and has not been submitted to another organization or for any other degree, except perhaps properly cited quotations and summaries.

Signature:

Name: Ammar Maythem Faisal

Date:     /     /2022

## COMMITTEE REPORT

We certify that we have read this thesis titled " **EXPERIMENTAL AND NUMERICAL STUDY TO INCREASE THE EFFICIENCY OF THE PHOTOVOLTIC THERMAL SYSTEM USING PCM**" submitted by **AMMAR MAYTHEM FAISEL** as examining committee, examined the student in its contents. In our opinion, the thesis is adequate for an award of the degree of Master degree of Technical Thermal Engineering.

Signature:

Name: **Dr. Ali Najah Kadhim**

Title : Assistant Professor

(Supervisor)

Date: / / 2022

Signature:

Name: **Dr. Ahmed.H.Ali**

Title : Assistant Professor

(Member)

Date: / / 2022

Signature:

Name: **Dr. Hayder Azeez Diabil**

Title : Assistant Professor

(Member)

Date: / / 2022

Signature:

Name: **Dr. Audai Hussein Kadhum**

Title : Professor

(Chairman)

Date: / / 2022

### **Approval of the Engineering Technical college – Najaf**

Signature:

Name: **Ass. Prof. Dr. Hassanain G. Hameed**

Dean of Engineering Technical college – Najaf

Date: / / 2022

## SUPERVISOR CERTIFICATION

I certify that this thesis entitled " **EXPERIMENTAL AND NUMERICAL STUDY TO INCREASE THE EFFICIENCY OF THE PHOTOVOLTAIC THERMAL SYSTEM USING PCM**", which is submitted by **AMMAR MAYTHEM FAISEL**, has been prepared under my supervision at the mechanic Techniques Engineering of Power Department, Engineering Technical College-Najaf, AL-Furat Al-Awsat Technical University, as partial fulfilment of the requirements for the Master degree of Technical Thermal Engineering.

Signature:

Name: **Dr. Ali Najah Kadhim**

(Supervisor)

Date: / / 2022

In view of the available recommendation, I forward this thesis for debate by the examining committee.

Signature:

Name: **Dr. Ahmed Salim Almurshdi**

(Head Mechanical. Eng. Tech. of

Power Dept.)

Date: / / 2022

## LINGUISTIC CERTIFICATION

This is to certify that this thesis entitled “” was reviewed linguistically. Its language was amended to meet the style of the English language.

Signature:

Name:

Date:

## **ACKNOWLEDGEMENT**

I would like to extend my deep respect and gratitude to the supervisor Dr. Ali Najah Kadhim for his support during the research period and his guidance to complete this study.

I extend my sincere thanks to the Dean (Ass. Prof. Dr Hassanain G. Hameed) of the Technical College of Engineering, Najaf, and the esteemed head of Mechanical. Eng. Tech. of Power Department (Dr. Ahmed Salim Almurshdi) to provide possible assistance to facilitate the study process. Special thanks go to the members of the Department for their assistance. Thanks to my dear parents, brothers and wife for their patience, support and encouragement throughout my life.

**Ammar Maythem Faisal**

2022

## **ABSTRACT**

Over the past century, several basic and applied fields of research have been driven by the desire to produce power from renewable resources. The use of photovoltaics, sometimes known as PV, is a straightforward and sophisticated way to capture solar energy which regards as one of the best options for renewable energy with no noise, pollution, or moving parts, PV devices (solar cells) are unusual in that they convert incident solar energy directly into electricity, making them strong, dependable, and long-lasting. The Reduced energy conversion efficiency of PV cells, which further failures over the operating time by raising the temperature of the cell above a particular limit, is one of the most significant challenges in employing solar systems. The electrical efficiency of PV modules is often reduced by 35% by the sun's irradiance reflecting off the panel.

The study was conducted at the Technical College of Najaf, Above the ceiling of the building of the Department of Mechanical Engineering Techniques of Power, Najaf / Iraq during the May in 2022, in terms of the effect of (change of factors and weather conditions, mass of PCM).

During this study, the benefit of adding a phase-changing material under the solar cells for the purpose of cooling and benefiting from the stored energy during the night was verified, thus increasing its efficiency and increasing the resulting energy. The study was in two parts, practical and numerical, through which three models were tested (PV, PV-TE, PV-PCM-TE). Numerically, the phase change material was tested for several types (SP-31, SP-50, SP-58, SP-70, SP-90), where SP-31 was the best thermal performance. Based on the practical tests that were conducted for 24 hours in the month of May for the three units, the resulting capacity of the PV,

PV-TE, PV-PCM-TE was (365 ,369 ,375) mW . As for the efficiency, of (14.58, 14.65, 14. % ) was recorded, respectively. The electricity which has been generated from the PV-TE, PV-PCM- TE during the day was 62,42 mV and at a rate of 10.1 and 6.8 mV at night respectively, this energy which has been generated at night can be used for sensors, accurate screens and some other applications.



## Contents

DECLARATION .....	I
COMMITTEE REPORT.....	II
SUPERVISOR CERTIFICATION .....	III
LINGUISTIC CERTIFICATION .....	IV
ACKNOWLEDGEMENT .....	V
ABSTRACT .....	VI
List of Figure.....	XI
List of tables.....	XIII
CHAPTER ONE INTRODUCTION .....	1
1.1 General .....	1
1-3 Photovoltaic panels types.....	4
1-5 Phase. Change. Material (PCM) .....	6
1-6 Photovoltaic panels cooling techniques .....	7
1-7 Problem Statement.....	9
1-8 Object of Research.....	10
1-9 The Scope of the Study .....	10
Chapter Two Literature review .....	12
2-1 General.....	12
2-1-1 Air Based PVT.....	12
2-1-1 Water based PVT .....	22
2-1-3 PCM-Based PVT Collectors .....	24
2-1-4 Thermoelectric (PV-TE) Hybrid Systems .....	25
2-3 PCMs and The Many Sorts of PCMs.....	26
2-3-1 Types of PCMs .....	27
2-3-2 Organic PCM.....	27
2-3-3 Inorganic PCMs .....	29
2-4 TE (Thermal Electric Device).....	31

CHAPTER THREE.....	44
3.1 Introduction.....	44
3.2 Model Geometry Proposed .....	44
3.2.1 PV Reference (PVREF Module) .....	44
3.2.2 PV with PCM (PVT-PCM) .....	45
3.3 Numerical Simulation of Proposed Modeling.....	46
3.3.1 Governing Equations.....	48
3.3.2 PV Cell Efficiency.....	49
3.4 The CFD model.....	50
3.4.1 Computational Fluid Dynamics software COMSOL Multiphysics .....	50
3.4.2 Model Geometry.....	50
3.4.3 Use of COMSOL Multiphysics Mesh independency check .....	51
3-5 Code Validation .....	53
Chapter Four .....	56
4-1 Introduction.....	56
4-2 System components .....	56
4-2-1 The photovoltaic panel .....	59
4-2-2- Thermal Electric Device.....	60
4-3 Heat sink .....	61
4-2-4 Aluminum Container .....	62
4-2-5 PCM Preparation .....	63
4-2-6 Thermal Preparation .....	63
4-3 Measurements .....	64
4-3-1 Temperatures .....	64
4-3-2 Solar radiation.....	65
4-3-4 Wind Speed.....	65
4-3-5 PV Module Analyzer .....	66
4-4 Process of conducting the experiment .....	67
Chapter Five .....	69
5.1 General .....	69
5.2 Theoretical results .....	69

5-2-1 Verification Model.....	69
5-2-2 Surrounding conditions and work site .....	69
5-2-3 Effect of PCM mass.....	71
5-2-4 Change State of The PCM Material from Solid to Liquid with Time .....	73
5-2-5 Power output and efficiency .....	75
5.3 Experimental results.....	76
5.3.1 Atmospheric Conditions Practically Measured By Measuring Instruments .....	77
5-3-2 Effect of Adding a Phase Change Material on the Temperature .....	79
5-3-3 Effect of adding phase change material on the efficiency .....	80
5-3-4 Effect of adding phase change material on the power .....	81
5-3-5 The effect of adding TE to generate electricity at night .....	82
5-3-6 I-V and P-V Curves .....	84
5-5 Cost Analysis .....	86
CHAPTER SIX.....	87
6.1 Conclusion .....	87
6.2 Recommendations .....	88
REFERENCES.....	89
APPENDIX - A.....	98
THERMOCOUPLE’S CALIBRATION.....	99
APPENDIX - B.....	103
WIND SPEED CALIBRATION .....	103
Appendix-C. Solar Meter Calibration:.....	104
Appendix-D LIST OF PUBLICATIONS .....	105
الخلاصه.....	110

## List of Figure

Figure (1.1) heliostat solar collector [1] .....	2
Figure (1.2) parabolic collector [1] .....	2
Figure (1.3) PV panels installation [2].....	4
Figure (1.4) [1] Photovoltaic panels .....	5
Figure (1.5) Thermoelectric generators (TEGs) [6].....	6
Figure (1.6) PCMs absorb and release energy [6] .....	7
Figure (3.1) Schematic diagram of PVREF module.....	45
Figure (3.2) Schematic diagram of PVPCM module.....	45
Figure (3.3) heat transmission pathways to and derived from the (PV/PCM) systems .....	47
Figure (3.4) Different types of meshing for PV module.....	52
Figure (3.5) Mesh at a mid-height cross section of the numerical model. ..	52
Figure (3.6) Mesh stability test .....	53
Figure (3.7) The simulated results of solar cells temperatures during the test day for PVREF. ....	54
Figure (4.1) Schematic diagram of the PV module cooling system with its all parts .....	57
Figure (4.2) The device while working during the day ....	<b>Error! Bookmark not defined.</b>
Figure (4.3) Photovoltaic module.....	59
Figure (4.4) Thermal electric module.....	60
Figure (4.5) Heat sink module .....	62
Figure (4.6) aluminum container .....	62
Figure (4.7) PCM Precision Parts .....	63
Figure (4.8) Thermal Grease Paste .....	64
Figure (4.9) Thermocouples and data logger.....	65
Figure (4.9) Solar radiation measurement device (Pyranometer).....	65
Figure (4.11) Air flow meter device (anemometer).....	66
Figure (4-12) PROVA 200A Solar module analyzer.....	67
Figure (5.1) A Temperature change over time.....	70
Figure (5.1) B. Wind Speed over time .....	70
Figure (5.1) C. Soler radiation over time .....	71

Figure (5.2) A- Effect of PCM (SP-31) mass .....	72
Figure (5.2) B- The relationship between temperature of PV and type of PCM .....	73
Figure (5.3) Stages of transformation of the PCM during the day .....	74
Figure (5.4) Variation of power with and without PCM. ....	75
Figure (5.5) Variation of efficiency with and without PCM. ....	76
Figure (5.6) Solar radiation changes during daylight hours. ....	77
Figure (5.7) Wind speed changes during daylight hours .....	78
Figure (5.8) Ambient temperature changes during daylight hours.....	78
Figure (5.9) shows the Temp. of the three models and ambient Temp. ....	79
Figure (5.10) Effect of adding phase change material on the efficiency ....	80
Figure (5.11) Effect of adding phase change material on the power.....	82
Figure (5.12) Electricity generation by TE device.....	83
Figure (5.13) Electricity generation at night.....	84
Figure (5.15) Comparison of the solar cell's Current-Voltage curves.....	85
Figure (5.16) Comparison of the solar cell's Power-Voltage curves.....	85
Figure A1. The calibration certificate by the manufacturer for thermocouples .....	99
Figure A2. Thermocouple's calibrations and data logger.....	100
Figure A3. T1 thermocouples calibration.....	100
Figure A4. T2 thermocouples calibration.....	101
Figure A5. T3 thermocouples calibration.....	101
Figure A6. T4 thermocouples calibration.....	102
Figure B1 Anemometer Calibration.....	103
Figure C1 solar meter calibration (Pyranometer) .....	104

## **List of tables**

Table (1-3) PV panel material properties [62] .....	47
Table (2-3) Thermophysical properties of PCM [63] .....	48
Table (3-3) Code Validation .....	54
Table (4-1) Photovoltaic specifications .....	59
Table (4-2) Thermal electric specifications .....	60
Table (4-3) Heat sink specifications .....	61
Table (5-1) materials Cost.....	86

## NOMENCLATURE

<b>Symbol</b>	<b>Definition</b>	<b>Unit</b>
<i>PV</i>	Photovoltaic	-
<i>PVT</i>	Photovoltaic thermal	-
<i>TE</i>	Thermoelectric device	-
<i>PCM</i>	Phase change material	-
<i>T<sub>r</sub></i>	reference temperature	°C
<i>η<sub>el</sub></i>	electrical efficiency	%
<i>η<sub>th</sub></i>	Thermal efficiency	%
<i>η<sub>r</sub></i>	reference efficiency	%
<i>β</i>	temperature coefficient	0.0045 °C <sup>-1</sup>
K	Boltzmann constant	$1.38 \times 10^{-23} \text{ m}^2 \text{ kg s}^{-2} \text{ K}^{-1}$

## CHAPTER ONE

### INTRODUCTION

#### 1.1 General

As the world population is growing by the day, its energy need is growing too. therefore many various types of fuel have been employed as a source of energy over the years. fossil fuels have been the dominant sources of energy for numerous years. The earth atmosphere began to alter in the previous century as a result of pollution and global warming caused by carbon dioxide generated by these fuel types. Humanity has begun to search a new source of energy that is both efficient and sustainable, as well as renewable, in recent years. Alternative fuels have been employed in a variety of ways, with solar energy being the most popular. Solar energy may be used both indirectly and directly, for example, by wind or geothermal energy [1]. Solar energy may be utilized to heat water in solar collectors and generate electricity in concentrated thermal collectors such heliostats, Fresnel collectors, and parabolic collectors (Figures 1.1 and 1.2). [1] Furthermore, direct photovoltaic panels convert light photons in solar radiation directly into electrons in a semiconductor, resulting in electrical power generation. When the solar radiation surpasses  $1000 \text{ W/m}^2$ , the power conversion in all forms of these panels ranges from 15% to 20% of the total falling radiation due to the produced materials and the issue of the surface working temperature increasing [2]. The two most common varieties of solar panels used in homes and businesses are monocrystalline and polycrystalline photovoltaic panels. As the poly-crystalline cells are easy to manufacture



therefor, it is cheaper to produce. The poly-crystalline cells' efficiency is less than the monocrystalline cells with a 12-15% conversion ratio from the total radiation fallen directly on the solar cell

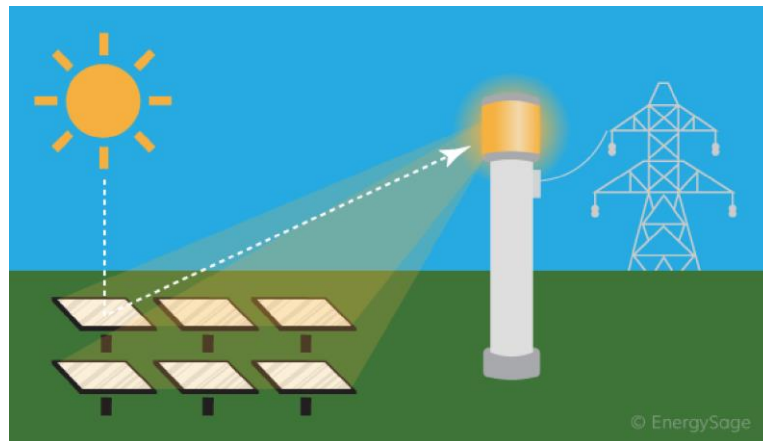


Figure (1.1) heliostat solar collector [1]

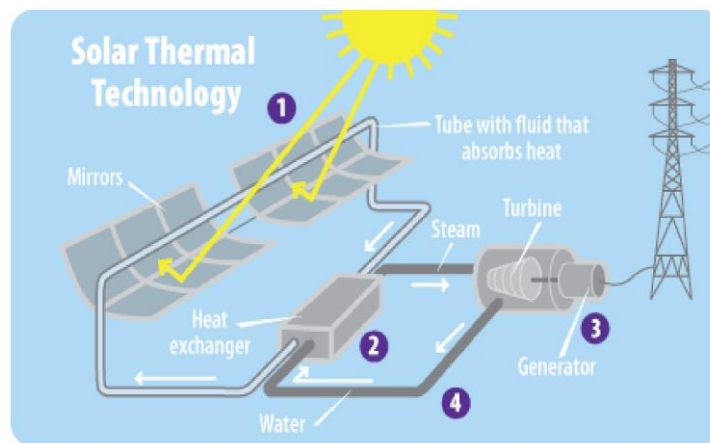


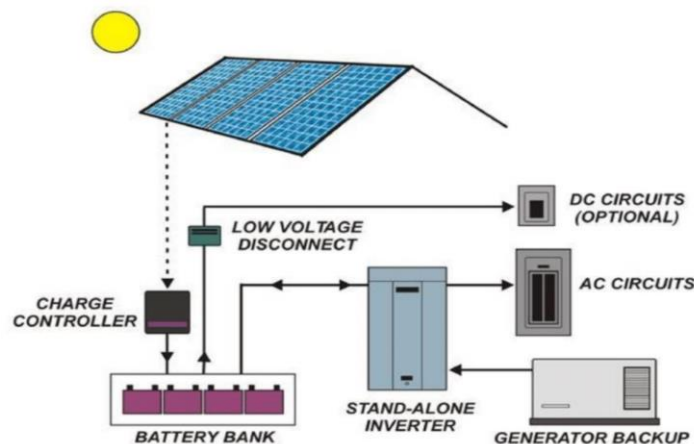
Figure (1.2) parabolic collector [1]

## 1-2 Research Background

The photovoltaic panel is a technology that directly converts solar energy into light via a phenomenon known as the photovoltaic effect. In 1839, a French scientist named Edmond Becquerel was the first to discover the photovoltaic phenomenon [2]. It was not employed in satellite applications until the 1960s, when it became the first. Photovoltaic panels exist in a variety of forms and sizes, but they always generate energy using a semiconductor.

The photovoltaic panel is made up of several layers, each of which serves a different purpose. With two semiconductors (P-type and N-type) coupled in a junction field, the semiconductor layers are the most crucial.

Due to the availability of silicon semiconductors, photovoltaic panels are becoming more popular as local and worldwide power sources. Furthermore, because photovoltaic cells are solid units (Figure 1.3), they may be simply joined to other groups of cells without moving components, making them suitable for usage in both home and industrial settings.



### Figure (1.3) PV panels installation [2]

The first industrial use of the photovoltaic panels was in the 1980s, and the installed capacities started to rise from 77 MW in the United States in 1996. The installed capacity increased to 100 GW in China in 2016, and the installed capacities around the world were growing fast so that the global power production in the time of this study, reaching 653 GW. According to the IEA, the global photovoltaic capacity will be around 4.7 TW (4674 GW) by 2050 [3]. The photovoltaic panel technology has reached a maximum power conversion (solar radiation into electricity) efficiency of 20% in industrial applications. Moreover, that conversion efficiency drops with the panel surface working temperature increase. Also the efficiency drops in about 0.5% for each 1C° above the 25 °C [4]. For that reason, a decent amount of that energy was wasted due to the panel surface overheating. Therefore, too many techniques have been used to reduce the panels surface working temperature.

#### **1-3 Photovoltaic panels types**

Two thin layers of semiconductors, most often silicon, make up photovoltaic cells. When a semiconductor is exposed to light, electrical changes in the molecules create electrons, which may be carried through conductors as a direct current collection (DC). Because a single cell power output is little, multiple cells are joined to make a string that is inadequate to be utilized. Direct current is generated and the cells are joined and coated to produce a solar panel. The PV panels are then linked in parallel or series to the glass layer Creating the appropriate voltage. current Photovoltaic panels are available in a variety of forms and sizes, depending on the

application. Researchers have generally split the evolution. There are three technological generations of photovoltaic systems, but there are three generations of photovoltaic systems. Both household and commercial photovoltaic panels are available. This term is often used. as seen in Figure (1.4) [1].

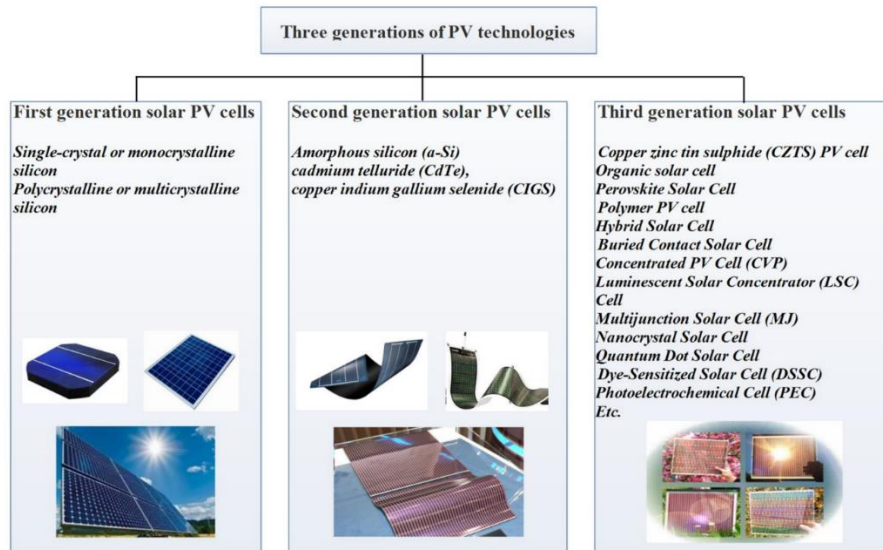


Figure (1.4) [1] Photovoltaic panels

#### 1-4 Thermoelectric device

The search for a new form of energy is a pressing issue as the energy crisis and environmental issues worsen. There has been a lot of attention in recent years in creating renewable energy. Thermoelectric generators (TEGs) are a promising environmentally friendly method of energy conversion since they directly convert heat to electricity using the Seebeck effect. Since they first appeared in the 1960s, useful TEG devices have advanced to the point where many manufacturers still provide TE modules for cooling power generation applications. Because of their unique benefits, such as their lack

of noise, pollution, mechanical vibration, and other characteristics [5]. The thermoelectric unit generates electricity from heat directly. The thermoelectric unit consists of two different materials connected at their ends: type N (with negative charge carriers) and type P (with positive charge carriers) the current flows when the electric is when there is a difference in temperature between the two ends of the device Figure (1.5) [6].

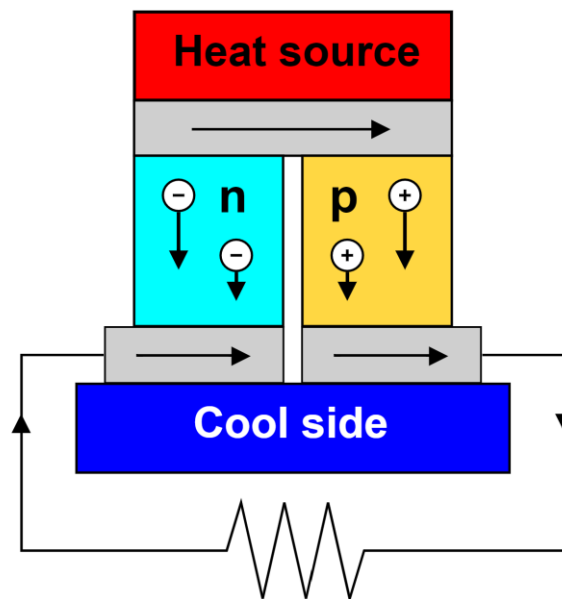


Figure (1.5) Thermoelectric generators (TEGs) [6]

### 1-5 Phase Change Material (PCM)

It is a substance that releases or absorbs energy for the purpose of changing from one state to another (solid to liquid or vice versa) and the phase transition may also be between non-classical states of matter, such as matching crystals. Through melting and solidification at temperatures, PCM is able to store and release large amounts of energy compared to storing ordinary heat. Where heat is absorbed or released, when a solid

substance changes to a liquid and vice versa, or when the internal structure of the substance changes. There are two types of PCM: the first is Organic substances derived from animals, plants or petroleum and the second is Salt hydrates, which are usually marine salt deposits. Phase change materials have the potential to gradually reduce the cost of renewable electricity. When using PCM, it must be wrapped so that it does not leak during its transformation from one state to another as shown in figure (1.6) [7]

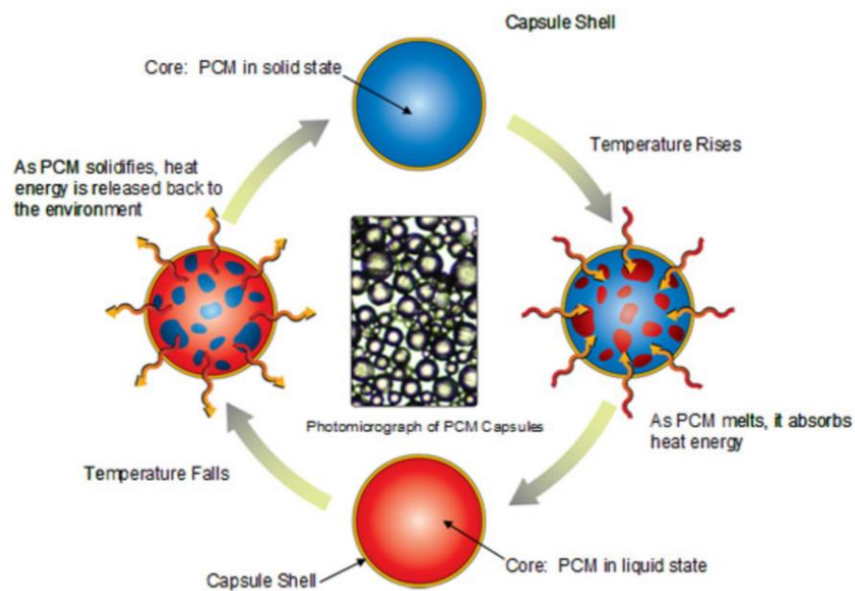


Figure (1.6) PCMs absorb and release energy [6]

### 1-6 Photovoltaic panels cooling techniques

Several researchers have investigated many techniques to cool these panels and keep them functioning close to the standard working temperature, utilizing various working fluids in various mechanisms, in order to decrease PV module cooling techniques classified in two general methods [8] :

#### A- Active cooling:

PV active cooling improve the transfer of heat between the PV module and the cold source by using external power. Active methods of cooling often used

- (1) Water spray on or under the PV.
- (2) Jet cooling Impingement.
- (3) The passage of air or water through channels or ducts through PV back surface.

### **B- Passive cooling**

Other types of cooling strategies, such as passive approaches, do not require an external energy source and do not require additional power usage.:

- (1) Thermosyphon technique.
- (2) Cooling of the submerged water.
- (3) Buoyancy-induced airflow.
- (4) Heat dissipater/sink of heat.
- (5) Phase change materials (PCM).
- (6) Technique of evaporative cooling.
- (7) Cooling by using wick made from cotton.
- (8) Heat pipe concept.

Active cooling techniques for PV are more efficient than passive ones, however passive cooling has historically been preferred due to considerations including low operating costs, high reliability due to little operational risk, and environmental friendliness [8].

## 1-7 Problem Statement

The development of solar panel technologies that have concentrated on boosting the efficiency of the solar panel has recently been the subject of extensive scientific research and manufacturers' attention. The conversion ratios of various types of solar panels vary. The silicon-based cells, nevertheless, are the most effective, converting up to 20% of the radiation energy. The remaining energy will either be reflected or transformed inside the panel itself into heat.

The effectiveness of the solar cell and, consequently, the amount of power it produces, are influenced by a number of factors. The key factors influencing the efficiency of the solar cell are the operating temperature and reflection losses. Under typical test conditions of 1000 W/m<sup>2</sup> incident radiation and 25 °C ambient temperature, all photovoltaics were created to function. As the temperature rises, the overall efficiency of the solar panel decreases by 0.4-0.5% for every 1°C above 25 °C. High levels of reflection in solar cells cause a loss of roughly 35% of incident energy, lowering power production and consequently solar cell performance. And also, one of the most important problems is the interruption of electricity generation from solar cells at night, so the most important problems can be solved as follows:

- 1- No electricity can be generated at night.
- 2- The solar cell's low efficiency and rising temperature during the day.
- 3- The high cost of batteries that store electricity.



### **1-8 Object of Research**

This study numerically and empirically investigates the effect of photovoltaic panel cooling on the efficiency and power output. The research methodology is based on a direct comparison between the traditional and improved photovoltaic panels by changing some parameters, and it also looks for the possibility of generating electric power at night depending on the heat stored inside the phase-changing material and can be summarized as follows:

- 1- To develop numerical models of the photovoltaic thermal collectors (PVT).
- 2- To generate electricity at night, depending on radiative cooling.
- 3- To increase the efficiency of the solar cell by adding PCM.
- 4- To reduce the costs by attaching sensors and small lights directly to the cell without using a battery.

### **1-9 The Scope of the Study**

This study investigates the numerical and experimental effects of photovoltaic panel cooling on switching efficiency and power output. The research methodology is based on a direct comparison between traditional and improved photovoltaic panels by changing some parameters and also the possibility of generating electricity at night depending on space cooling and can be summarized as follows :

- 1- Reducing the effect of heat on the performance of a silicon solar cell.
- 2- Increasing the energy generated by cooling the bottom of the cell.
- 3- presenting the change of weather conditions on the performance of the solar cell.

5- Increasing the possibility of generating electricity at night and compare the PV-TE, PV-PCM-TE cells.

## **Chapter Two**

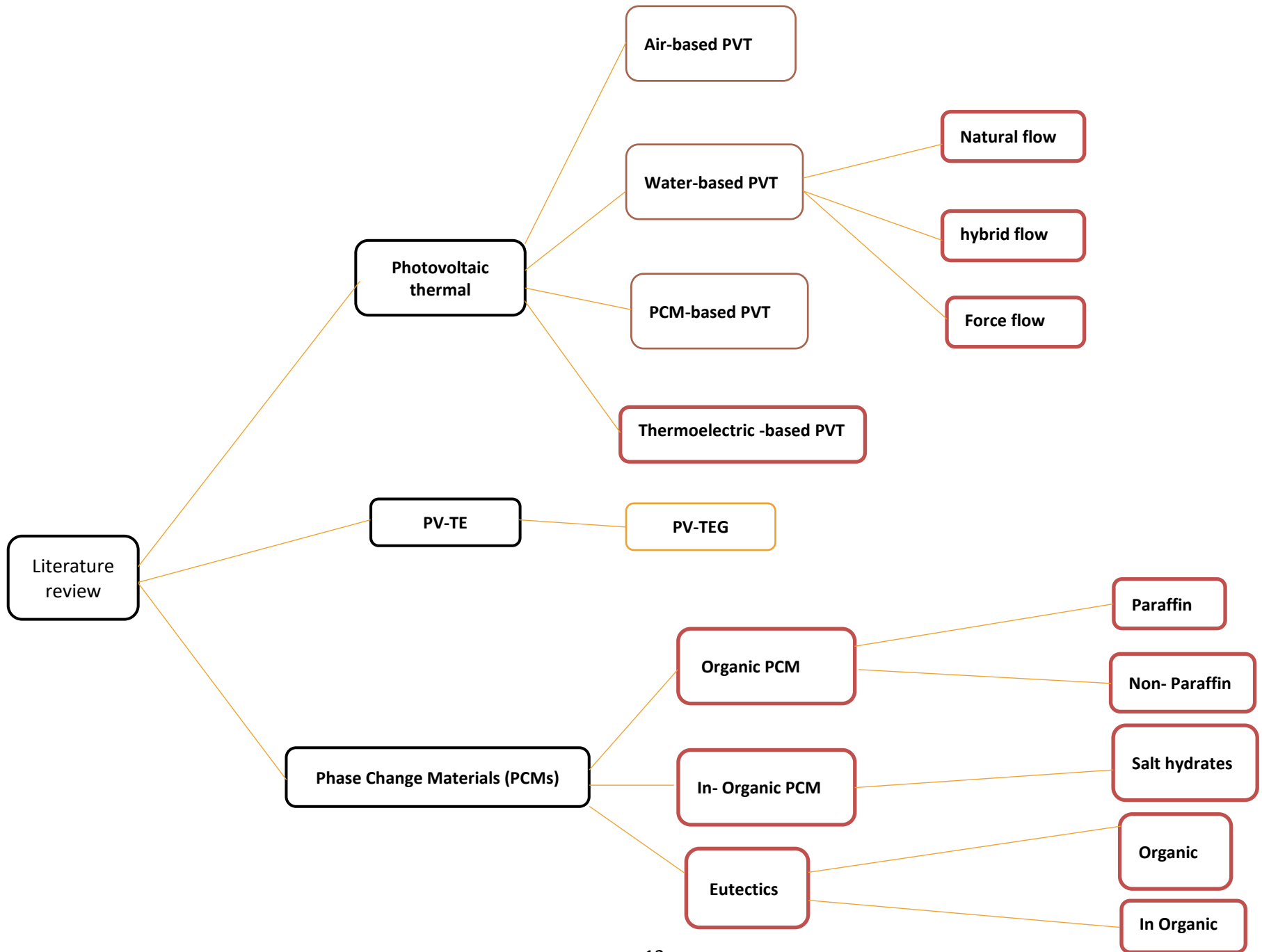
### **Literature review**

#### **2-1 General**

A solar thermal system consists of two parts: a solar module and a heat dissipation component that cools it. This technology has the ability to generate electrical and thermal energy at the same time. As a result, the PVT system has better overall efficiency than the PV system. In the PVT system, improving the optical properties of the working fluid can improve efficiency. In other words, the best performance of the PVT system, the higher the transmittance of visible light and solar infrared rays absorbed.

##### **2-1-1 Air Based PVT**

Air is one of the most important natural factors affecting heat transfer, and air is relied on to cool cells. Some previous researches will be discussed on how to take advantage of air cooling.



**Rounis et al. [2016]** [9], presented the findings of a numerical study comparing the performance of BEP/T systems in their study. The investigation was conducted on a chilly winter day, a hot summer day, and in various conditions. A multiple-inlet BIPV/T system was found to have up to 1% higher electrical efficiency, equal to 7% more power added to a 120-kW system total output, and up to 24% higher thermal efficiency, while resulting in the lowest and most uniform PV temperatures.

**Juwel Chandra [2016]** [10], designed a BVT solar collector system with a single antenna and a number of thin rectangular fins to disperse heat. A fin system fused by a thin flat metal plate was employed to examine the performance of TFMS. The temperature parameters were then monitored and compared to a number of other methods and configurations. The highest thermal efficiency and PV efficiency were found to be around 56.19 % and 13.75 %, respectively.

**Mohamed El Amine Slimani (2016)** [11], was looking at the possibilities of including the formation of a hybrid photo-thermal solar collector in an indirect way. A study of the solar drying system has been conducted. The air goes via a double corridor below and above the photovoltaic unit in the existing layout of a solar photovoltaic/thermal air collector. The results showed that the electrical, thermal, and total energy efficiencies were 10.5 %, 70 % and 90 %, respectively. The findings of this study also showed how significant the influence of certain factors and operations was conditions affecting the hybrid complex's performance .

**Ahmad Fudholi (2018)** [12], The performance of a PVT collector with -groove was calculated using a mathematical model and compared to

experimental results. To solve the temperature equation for each PVT system element, a matrix inversion method was used. The results of the mathematical model are 94 % accurate when compared to experimental data. For theoretical and experimental research, the average PVT energy efficiency is 65.52 percent and 66.73 %, respectively. For theoretical and experimental research, the average PVT exergy efficiencies are 12.91 % and 12.66 %, respectively. For solar radiations of 385 and 820 W/m<sup>2</sup>, the average IP is 173 and 369 W, respectively.

**S. Senthilraja (2020)** [13] , aims to identify the performance of the solar collector (thermal photovoltaic) hydrogen production system. The water splitting system is manufactured with the help of solar energy. The results were an increase in the energy output with an increase in the flow rate and the highest thermal efficiency 33.8% and electrical efficiency 8.5%.

### **2-1-1 Water based PVT**

Air cooling fails to accommodate the temperature rise at the surface of PV cells at high working temperatures, resulting in a crucial loss in conversion efficiency. Cooling with liquid coolant as heat provides a superior alternative to air cooling. extraction medium to keep the temperature of the machine at the correct level PV cells and a more efficient use of collected thermal energy.

**Ning Xu, Jie Ji (2016)** [14] , this research looks at the characteristics of a high-concentration photovoltaic/thermal (HCPV/T) module with a point-focus Fresnel lens. Numerical approaches are used to create the module's electrical and thermal models. The thermal model is based on a two-dimensional steady-state heat transfer model, whereas the electrical model

is based on the Shockley diode equation. The models take into account the effects of environmental conditions and coolant water. Irradiance, ambient temperature, wind speed, water temperature, and mass flow rate are the models' inputs. Electrical and thermal efficiency are the most common outputs. When the simulated and experimental data are compared, there is a lot of agreement. The HCPV/T module has a 28 % electrical efficiency and a 60 % thermal efficiency, according to the results. Solar irradiation, not cell temperature, has the greatest impact on electrical efficiency. The thermal efficiency improves as irradiance, ambient temperature, and water mass flow rate rise. Increased water temperature and wind speed, on the other hand, will reduce thermal efficiency. In addition, the HCPV/T module can provide hot water up to 70 C without significantly reduction in electrical efficiency.

**Mawufemo Modjinou (2016)** [15] , the authors devised and built an unique micro-channel heat pipe array using a crystalline silicon (c-Si) solar photovoltaic/thermal system (MHP-PV/T). To produce electrical and thermal energy concurrently, the proposed design configuration integrated c-Si solar cells with broad micro-channel heat pipes (MHP) that were filled with a prescribed amount of acetone as refrigerant under a vacuum condition in the same insulated frame. The MHP-PV/heat T's and mass transfer properties were examined using both numerical and experimental methods. MATLAB was also used to investigate the heat pipe's transient behavior and parametric heat transfer constraints. The thermal instantaneous efficiency and the lowered temperature parameter were shown to have a linear relationship. With a 70 W electrical power output, the greatest instantaneous efficiency was found to be 54.0 %. The daily

thermal and electrical efficiencies were 50.7 % and 7.6 %, respectively, according to the findings. The MHP's transient behavior displays a faster thermal reaction to heat input in the 48.8–49.2 °C temperature range and a slower response when the thermal diffusivity is decreased to 0.05 cm<sup>2</sup>/s.

**Ruobing Liang (2017)** [16] , presenting a numerical model of a photovoltaic thermal collector and calculated the PV module temperature, as well as thermal and electrical efficiency, In the experimental investigation., the PV module temperature, and the absorber plate temperature of the PVT collectors in the intercept of the theoretical line is 3.6 % higher than the experimental line when the average temperature of the working fluid is equal to the ambient temperature, i.e. at maximum thermal efficiency, but the intercept of the electric experimental line is 5.8 % higher than the el, theoretical line. It means that the PVT collector's mathematical model is fairly accurate, as the theoretical and experimental results are nearly identical.

**Amira Lateef Abdullah [2020]** [17], the researcher talked about the experimental data that is employed in a program that simulates internal experimental trials. It was compared to a standard white board without a cooling system using the Fifty system. The greatest electrical efficiency was 10%, with 500 W/m<sup>2</sup>, and the thermal efficiency was 66%, with 500 W/m<sup>2</sup>, and then finished with it. The lower the temperature and the higher the electrical efficiency, the higher the flow rate.

### **2-1-3 PCM-Based PVT Collectors**

Changes in phase of PCMs are substances capable of absorbing and releasing enormous amounts of energy as latent heat via a reversible isothermal process at a specific phase transition temperature. Due to its



higher energy storage density within a smaller temperature range, latent heat storage with PCMs is better than sensible heat storage. Organic materials such as paraffin wax and fatty acids are classified as organics, inorganics such as salt hydrates are classified as inorganics, and eutectic mixtures of organic and inorganic PCMs are classified as eutectic mixtures of organic and inorganic .

**Taher Maatallah (2019)** [18] , in India, a study of the PVT-PCM/Water system was carried out under atmospheric circumstances. Experiments comparing the overall performance of PV energy and PVT-PCM water-based panels were done. The PVT-PCM/water system was studied under various external environmental conditions, and it was discovered that PCM integration improved heat and mass transfer. When compared to a conventional PV panel, the electrical efficiency of the new PV panel is 26.87 % and 40.59 %, respectively, with a 17.33 % increase in electrical efficiency. The water-based PVT-PCM system was discovered to have a payback time of roughly 6 years. It is 11.26 % shorter than typical PV panels in terms of total power.

**Ali Naghdbishi (2020)** [19] , the researcher evaluated the electrical and thermal performance of the system ( PVT\PCM) and compared the experimental results of the conventional photovoltaic unit (without thermal collector). The fluid increases the thermal energy efficiencies 23.5% and the electrical energy is 4.21% where there was a difference in temperature for the surrounding PVT surface.

#### **2-1-4 Thermoelectric (PV-TE) Hybrid Systems**

Thermoelectric (TE) modules are solid-state semiconductor devices that can convert heat energy to electrical energy or the other way around. Thermoelectric elements comprised of two different semiconductors, p- and n-type junctions, are coupled electrically in series and thermally in parallel to form a TE module.

**Dr. Vishal Verma (2013)** [20] ,in a building-integrated system, TE coolers were used to help cool PV modules. To evaluate the performance improvement of the TE coolers on PV, a dynamic model of the BIPV/TE system was built, taking PV panel temperature into account. To improve heat transfer, the BIPV/TE system includes a TE module attached to the back of the PV module and a heat sink linked to the other side of the module. The results demonstrated that the BIPV/TE combined system can function at 53 °C PV module temperature without losing PV power, allowing the module to be cooled down by 10 °C, extending the PV module's life and hence its performance.

**Jia Zhang (2020)** [21] ,it's also been proven that efficient heat transmission can help PV-TE hybrid devices work better. By removing the upper ceramic plate of conventional TE devices, a variety of unique integrated PV-TE hybrid devices with improved heat transmission characteristics were created in their study. To prevent an electrical connection between the PV cell and the TE device, an insulating layer was put on the back of the PV cell.

### **2-3 PCMs and The Many Sorts of PCMs**

PCMs are organic or inorganic substances that absorb a lot of energy from the sun. During the phase shift process, thermal energy is stored in these materials. When the solid to liquid and liquid to solid phases change, these

materials absorb and return thermal energy to the environment, respectively.

### **2-3-1 Types of PCMs**

PCMs are classified into three categories: organic, inorganic and eutectic. The temperature ranges of the PCMs and their thermal conductivity.

### **2-3-2 Organic PCM**

Paraffins and non-Paraffins are the two types of organic materials. Corrosive materials include organic materials with homogenous melting, core forming, and materials utilized as coatings. The organic PCMs used in building heating and cooling have a 20-32 C is the melting point.

**Tingyu Wang (2017)** [22] ,in this study, a new microcapsule-based phase change composite (PCC) with carbon network was designed to improve thermal conductivity and thermal stability. The theoretical ones were computed using the effective medium theory (ETM). Furthermore, an effective theoretical model was proposed and modified to estimate the thermal conductivity of such composites with various expanded graphite mass fractions (EG). As a result, with 24 wt. percent EG, the obvious denser carbon network structure of PCC was further confirmed, and the corresponding thermal conductivity was improved by up to 24 times that of virgin paraffin.

**Luo Jian-Feng (2015)** [23] ,by heating and compressing a mixture of squama expanded graphite (EG) and paraffin, composite phase change materials (PCMs) with high anisotropic thermal conductivity can be made. Numerical and experimental studies are conducted on the phase-change heat transfer properties of composite paraffin/EG PCMs. The phase change heat transfer model is simplified as a one-dimensional monolayer in the

numerical simulation, and the monolayer is heated by two stable heat fluxes on both sides. The PCM composite is placed in a metal box in the experiment, and the underside of the metal box is heated with an electric burner. A heat flow is discovered to be carried from the metal box's side wall to the cover board, which subsequently heats the composite PCMs. The numerical simulation confirms the experimental phenomenon. The experimental results reveal that the composite PCM's thermal conductivity is anisotropic, and that the temperature curves are deflexed and scattered throughout the apparent heat transfer process of the PCMs in liquid state. The numerical findings show that convection between the environment fluid and the aluminum cover board causes the above phenomena of deflexed and scattered temperature curves. With each other, the correctness of both the experimental and numerical methods is checked.

**Peizhao Lv (2016)** [24] ,in this research, the researcher used different particle sizes of kaolin to incorporate paraffin through the vacuum saturated nation method. The results showed that the paraffin/kaolin compound with the largest particle size of kaolin K4 has the highest thermal conductivity of 0.413 W/m. K at 20°C. Among the various compounds, the latent heat capacity of paraffin is 119.49 (J/g) and the temperature of change is 62° C. Storage clearance was studied.

**Qinrong Sun (2017)** [25] ,the researcher has developed a direct-number hybrid ( PEG/CMPs) composite ((PEG) methodology with high thermal conductivity for advanced thermal energy storage. The results prove that the thermal conductivity of the compound (PEG/CMPs) increases 65 % and the temperature of supercooling occurs at 6.5 °C during storage/cooling energy.

**Weixiong Wu (2019)** [26] ,in this research, a flexible, stable, thermally shaped PCM compound consisting of PA and OBC and EG is applied. The results presented in the work indicate that the prepared procession PCM has a potential application for heat and has the potential for energy storage and thermal management. There are three main factors that affect heating and cooling processes: thermal conductivity, natural convection, and latent heat absorption.

**Mohammd S .Yousef (2019)** [27] , studied the improvement of heat transfer properties in the PCM storage unit applied to the static solar energy system. Using cylindrical pin fins integrated in PCM, three cases were done, the first without PCM, the second with PCM, and the third with a solar stator with heat sink for the track fins built into PCM. The results for the distillates were 17% and 7% higher than the first case and the case second in a row.

**Ruchira N. Wijesena (2020)** [28], presents a new strategy for shape stabilization of liquid and solid phase change materials. Where the (PCM) materials were prepared based on the use of chitin nanofibers (CNFs) and the results indicated the stability of the shape of the compounds at 88% transmittance and it was seen that the (CNF) phase had an effect on the heat properties of the material (PEG-CNF) .

### **2-3-3 Inorganic PCMs**

Salt and metal hydrates are two types of inorganic compounds. In comparison to organic chemicals, inorganic compounds have a high latent heat per mass and volume, are cost-effective, affordable, and non-flammable. However, there are certain difficulties with these materials, such as undercooling and separation (which affect the properties of the phase

change). The following is the general principle of salt hydrates. Dehydration is the solid-liquid phase transition of salt hydrates. Salt hydrates are a particularly important class of PCMs with the following properties: Low latent heat per volume, but high latent heat per volume low volume changes during melting, strong thermal conductivity Toxicology, homogeneous melting, and the density differential with water are all factors to consider. (as a result of which it is dumped at the end of the case)

**W.Q. Li (2014)** [29] , the researcher deals with the thermal system of high energy (lithium-ion battery packs) using a sandwich structure combined with a copper foam impregnated with paraffin that was designed and experimentally realized, and the results showed that the temperature cannot be safe depending on the natural load while when using (PCM) maintains the temperature inside. The battery improves the effectiveness of thermal conductivity, at a rate of 1 to 3 degrees Celsius.

**Y.B. Tao ( 2015)** [30], this study discusses the possibility of enhancing the thermal performance of PCM salts of high-temperature carbonate, where four types of carbon nanomaterials were selected, the first is a nano-material with a specific surface area such as graphene, and the specific heat can be improved up to 18.57%, and the second is a nano-material with a vertical structure. The thermal conductivity was calculated. Up to 56.98 %, the third focuses on CPCM melting temperature transfer and enthalpy melting, and the fourth is nanomaterials additives that have a limited effect. The results showed that the second substance (SWCNT) is the optimal additive to enhance the thermal properties.

**Abid Hussain (2016)** [31] , an effective thermal management system for high-grade lithium-ion batteries using a new compound ((nickel foam-

paraffin wax) was studied and the results were compared for two cases, the first with natural air cooling and the second with PCM materials. The effect of PCM is high to reduce the temperature, as it showed a decrease in temperature by 31% compared to the first case, with an average of 2 degrees Celsius.

**Angela C. Evers (2020)** [32] , the researcher studied, developed and tested the insulation of cellulose reinforced with PCM for use in the walls of the frame, where he used two types of PCMs, paraffin-based and hydrated salt-based using two concentrations, the first 10% and the second 20% in 1.22 m of the frame cavity. The results showed that the PCM paraffin-reinforced insulation reduces the average peak temperature by up to 9.2%.

#### **2-4 TE (Thermal Electric Device)**

Using a thermoelectric generator is one promising option (TEG). Gas-free emissions, solid-state operation, maintenance-free operation without moving parts or chemical reactions, wide scalability, a long-life period of reliable operation, and minimal environmental impact are just some of the benefits of thermoelectric (TE) devices. As a result, combining PV and TE to create additional electricity could be considered. When a photovoltaic module and a solar thermoelectric generator are combined, photons outside the narrow absorption wavelength range of a specific solar cell can be directed to the TE modules, which create energy via the thermoelectric effect. This would boost energy conversion efficiency while lowering heat dissipation by the PV module.

**Ofer Beerli (2015)** [33], a hybrid PV-TEG demonstrator based on CMJ architecture was empirically and conceptually tested in this study. The hybrid system's efficiency reached 32 % using widely available MJ PV cells

and TEG. With increasing sun concentration and temperature, the direct electrical contribution of the TEG to the hybrid system's efficiency increases, reaching a maximum of nearly 20 % for a solar concentration of 300. When employing more modern PV cells and TE materials, further greater efficiency and power values are envisaged, with a real possibility of exceeding 50 % total efficiency.

**Rezania (2016)** [34] , a model of thermal photovoltaic hybrid panels (PV-TEG) was simplified, and the results showed that the radiant heat loss from the front surface and the convective heat loss due to wind speed are among the most important parameters in the performance of the hybrid panel, and (TEG) plays only a small role in energy and efficiency improved by 16.6% .

**Wei Zhu (2016)** [35] , the conductor ensures a significant temperature difference on both sides of the TE module. Because of the extra The designed PV-TE hybrid system accomplishes electrical generation attributed to thermoelectric generator. In the outside test, the peak efficiency was 23%, which is 25% higher than PV (photovoltaic) cells. Furthermore, the thermoelectric generator delivers an additional 648 J of electrical energy even when it is not in use.

**M. Benghanem (2016)** [36] , we conclude in this work that combining the thermoelectric device with the solar cells to produce a hybrid system will boost the efficiency of the solar cells.

The thermoelectric module is attached to the back side of the solar cells and is used to cool them. The effectiveness of solar cells increases by 0.5 percent every degree Celsius decrease in temperature as a result of this finding. The proposed hybrid PV/TEM system for PV applications in hot



areas provides good performance at a cost of roughly 6% of the total cost of traditional PV systems.

**Dianhong Li (2017)** [37], the researcher proposed a one-dimensional model to analyze the characteristics of photovoltaic cells (PV-TE) and the system (exergy and energy) was analyzed. The results show that the high concentration ratio used in the hybrid system (PV-TE) enhances the efficiency of the system, and when using type (CIGS) it increased by 21.6% and type (Thin film silicon) increased by 13.1%.

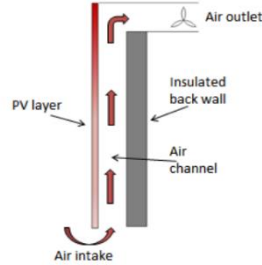
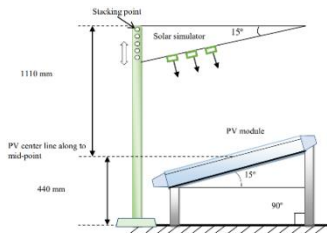
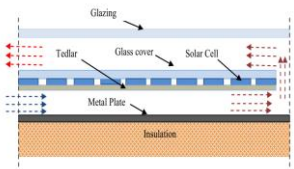
**Jin Zhang (2017)** [38], the resulting electrical energy efficiency of the hybrid system (PV-TE) is calculated and the energy losses resulting from the inability to reverse heat transfer, which are considered small, are calculated. The system is improved by controlling the water tools in the cooling blocks, and using the (PCM) system, and the results showed an increase in efficiency, reaching 19.1%.

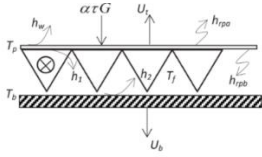
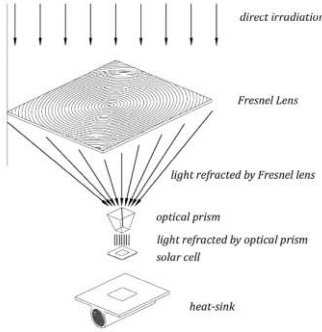
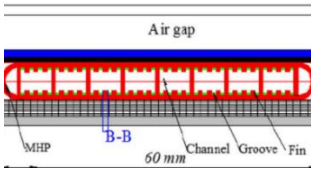
**Ershuai Yin (2017)** [39], this research discussed the thermal concentration ratio, where the effect of radiation change with time was neglected. The results showed that the ((PV-TE) coupling enables the system to obtain the highest average efficiency for one day by improving the concentration ratio. The efficiency ratio increased from 15.97% to 16.75%.

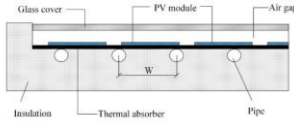
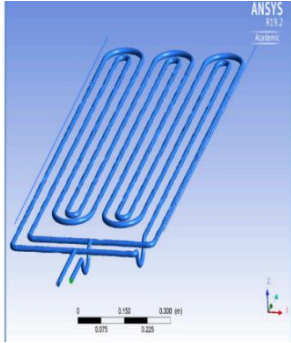
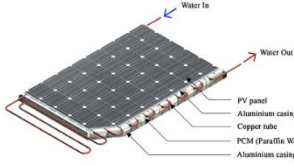
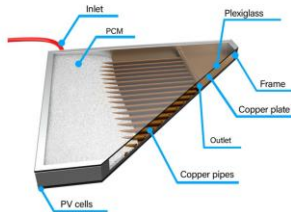
**R. Bjørk (2018)** [40], the researcher made a comparison between the independent PV of type (c-Si, a-Si, CIGS and CdTe) and the PV compound on it (TEG), where the photovoltaic efficiency was calculated by depending on the photovoltaic temperature and the efficiency value is approximately 34%.

**Guiqiang Li (2018)** [41], this study which relied on the internal electrical resistances for (TE), provided a knowledge of the maximum efficiency for (PV-TE) and the study was carried out using a cell (c-Si) and the results indicated that the highest resistance obtained for cell (c-Si) is 0.75 ohms and for cell (GaAs) is 2 ohms and the efficiency was 11.6%.

**Yi-Peng Zhou (2020)** [42], the researcher manufactured a device consisting of a coupling of several devices for the purpose of analyzing the advantages and disadvantages of the full solar spectrum. The comparison was made between the independent (PV) system and the (PV-TE) system, where experiments were conducted in the same surrounding atmospheric conditions due to the fluctuation of solar energy, where on the sunny day the strength of the system (PV-TE/T) increased by 11.6% for the tandem (PV-TE) system, and this percentage increased to 36.6% on a

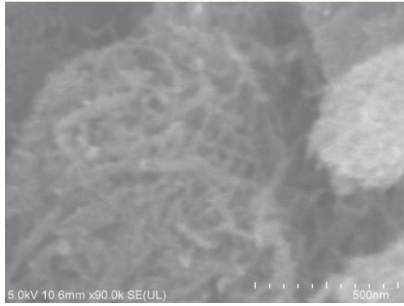
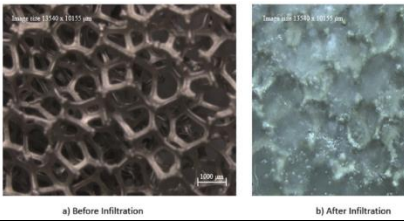
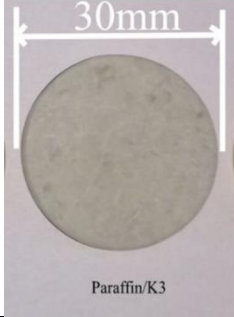
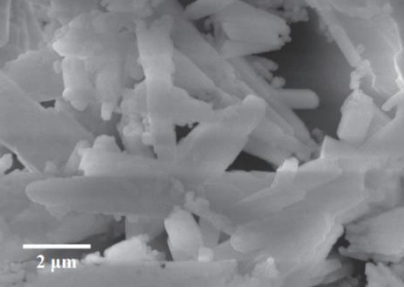
NO	Author	Electric efficiency%	Thermal efficiency%	Capture	Notes
<b>Air based PVT</b>					
1	<b>Rounis et al. [2016] [9]</b>	7%	24%		A multiple-inlet BIPV/T system was found to have up to 1% higher electrical efficiency.
2	<b>Juwel Chandra [2016] [10]</b>	13.75 %	56.19 %		A fin system fused by a thin flat metal plate was employed to examine the performance (TFMS)
3	<b>Mohamed El Amine Slimani (2016) [11]</b>	10.5%	70%		The numerical results show the energy effectiveness of this hybrid collector configuration and particularly its interesting use in an indirect solar

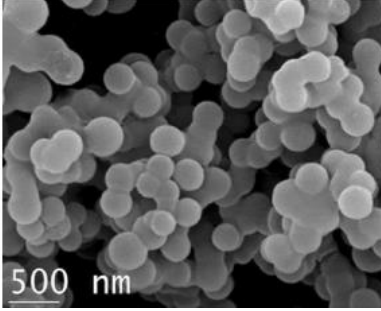

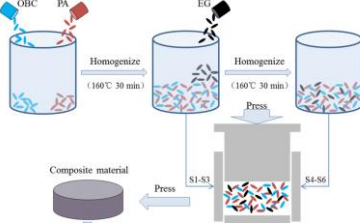
4	<p style="text-align: center;"><b>Ahmad Fudholi (2018) [12]Malaysia</b></p>	12.91%	65.52%		Improvement potential under solar radiations of 385 and 820 W/m <sup>2</sup> and mass flow rates between 0.007 and 0.07 kg/
5	<p style="text-align: center;"><b>Senthilraja (2020) [13] India</b></p>	8.5%	33.8%	-----	Study aims to identify the performance of the solar collector (thermal photovoltaic) hydrogen production system
<b>Water based PVT</b>					
6	<p style="text-align: center;"><b>Ning Xu, Jie Ji (2016) [14] China</b></p>	28 %	60%		The HCPV/T module can provide hot water up to 70 C without significantly reducing electrical efficiency
7	<p style="text-align: center;"><b>Mawufem o Modjinou (2016)[15] China</b></p>	7.6%	50.7%		The MHP's transient behavior displays a faster thermal reaction to heat input in

					the 48.8–49.2 °C temperature range
8	<b>Ruobing Liang</b> (2017) [16] <b>China</b>	14.25%	62%		TPV increases from 50.65 to 71.25 when the °C Ta rises from 0 to 30 °C
9	<b>Amira Lateef Abdullah</b> [2020][17] <b>Malaysia</b>	10%	66%		The increasing mass flow rate led to reduce the cell temperature and increase the electrical efficiency
<b>PCM-based PVT collectors</b>					
10	<b>Taher Maatallah</b> (2019) [18] <b>/ India</b>	26.87%	40.59%		Experiments comparing the overall performance of PV energy and PVT-PCM water-based panels were done
11	<b>Ali Naghdbishi</b> [2020] [19] <b>Iran</b>	4.21%	23.5%		Compared the experimental results of the conventional photovoltaic unit (without thermal

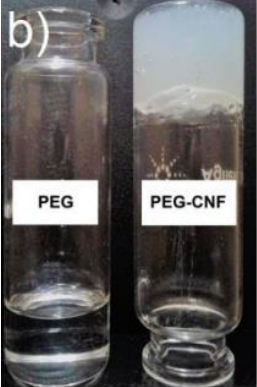

					collector)
<b>Thermoelectric (PV-TE) hybrid systems</b>					
<b>12</b>	<b>Dr. Vishal Verma</b> [2013] [20] India	-----	-----		allowing the module to be cooled down by 10 °C
<b>13</b>	<b>Jia Zhang</b> [2020] [21] China	-----	-----		This shows that PTE of the integrated hybrid device S2b is increased by 61.66% relative to that of S1b when 15 C cooling (C4)

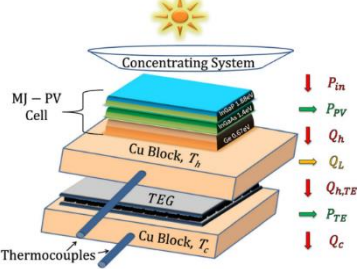
<b>PCM (Phase Change Material)</b>				
<b>No</b>	<b>Author (s) and work year / place</b>	<b>PCM used</b>	<b>Capture</b>	<b>Note</b>
<b>14</b>	<b>Luo Jian-Feng (2015)</b>	paraffin	-----	By heating and compressing a mixture (EG) and paraffin

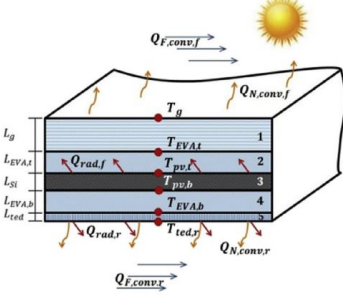
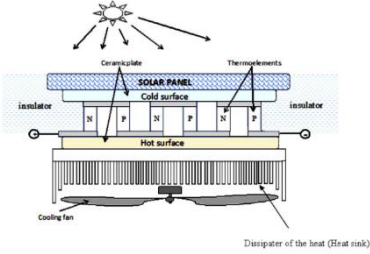
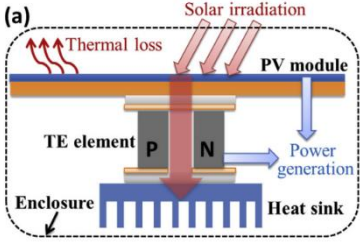
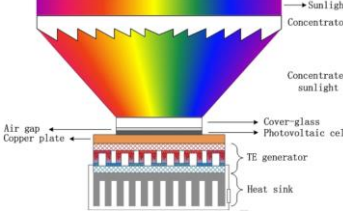
	[23] /China			
15	<b>Y.B. Tao (2015)</b> [30]/ China	carbonate salt		The thermal conductivity was calculated. Up to 56.98 %.
16	<b>Abid Hussain (2016)</b> [31]/ Hong Kong	nickel foam-paraffin		showed a decrease in temperature by 31% compared to the first case, with an average of 2 °C
17	<b>Peizhao Lv (2016)</b> [24]]/ China	paraffin/kaolin		the temperature of change is 62° C
18	<b>Tingyu Wang (2017)</b> [22]China	paraffin		thermal conductivity was increased by as much as 24 times of the pristine paraffin.

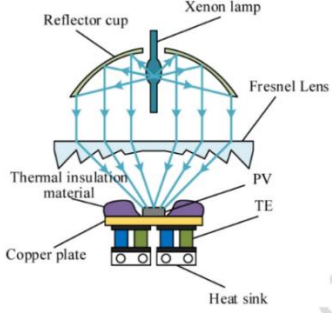
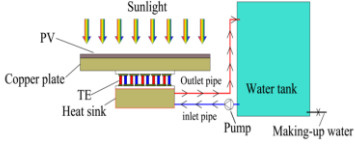
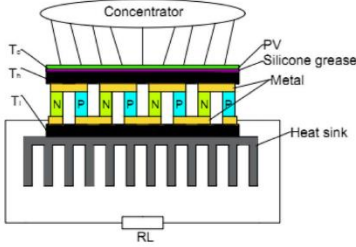
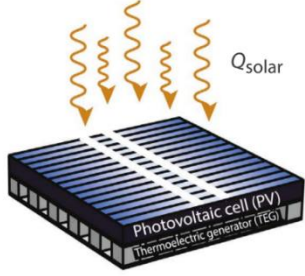
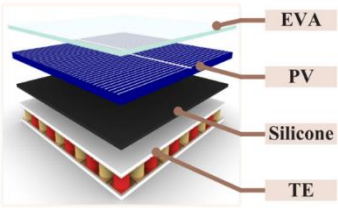
19	<b>Qinrong Sun (2017)</b> [25]/ <b>China</b>	polyethylene glycol (PEG)		The results prove that the thermal conductivity of the compound (PEG/CMPs) increases 65 % and the temperature of supercooling occurs at 6.5 °C during storage/cooling energy.
20	<b>Mohammad S .Yousef (2019)</b> [27]	Paraffin wax		(case 2) negatively reduces the daylight productivity by 7% with an enhancement in the overnight  (case 1). The total daily accumulated yield of freshwater of  (case 3) was greater than that of case 1 and case 2 by 17% and 7 %, respectively. Also,
21	<b>Weixiong Wu (2019)</b> [26] / <b>China</b>	-----		In this research, a flexible, stable, thermally shaped PCM compound consisting of PA and OBC and EG is applied



22	<b>Ruchira N. Wijesena (2020)</b> [28]/ Colombo	polyethylene glycol (PEG)		the stability of the shape of the compounds at 88% transmittance.
23	<b>Angela C. Evers (2020)</b> [32] / USA	hydrated salt		The results showed that the PCM paraffin-reinforced insulation reduces the average peak temperature by up to 9.2%

<b>TE (thermal electric device)</b>				
No	Author (s) and work year / place	efficiency	Capture	Note
24	<b>Ofer Beeri</b> 2015 [33]  China	32%		With a real possibility of exceeding 50% total efficiency.

25	<b>Rezania</b> 2016 [34] <b>Denmark</b>	16.6%		A model of thermal photovoltaic hybrid panels (PV-TEG) was simplified.
26	<b>M. BENGHANE</b> 2016 [36] <b>Saudi Arabia</b>	6%		The effectiveness of solar cells increases by 0.5 percent every degree Celsius decrease in temperature.
27	<b>Wei Zhu</b> 2016 [35] <b>China</b>	25%		The thermoelectric generator delivers an additional 648 J of electrical energy even when it is not in use.
28	<b>Dianhong Li (2017)</b> [37] <b>China</b>	21.6 % 13.1%		Using type ( CIGS) it increased by 21.6 % and type (Thin flim sillcon ) increased by 13.1%.

29	<p><b>Jin Zhang</b> 2017 [38] <b>China</b></p>	19.1%		The system is improved by controlling the water tools in the cooling blocks
30	<p><b>Ershuai Yin</b> (2017) [39] <b>China</b></p>	16.75%		The efficiency ratio increased from 15.97 % to 16.75%.
31	<p><b>Guiqiang Li</b> 2018 [41] <b>China</b></p>	11.6%.		The highest resistance obtained for cell (c-Si) is 0.75 ohms and for cell (GaAs) is 2 ohms.
32	<p><b>R. Bjørk</b> 2018 [40] <b>Denmark</b></p>	34%		PV of type (c-Si, a-Si, CIGS and CdTe).
33	<p><b>Yi-Peng Zhou</b> 2020 [42] <b>China</b></p>	36.6%		System (PV-TE/T) increased by 11.6% for the tandem (PV-TE) system, and this percentage increased to 36.6%.

## **CHAPTER THREE**

### **NUMERICAL SIMULATION**

#### **3.1 GENERAL**

The goal of this chapter is to create heat balancing equations for each component of each module and to utilize the COMSOL program V.5.5 to present, firstly, the heat transport mechanism and secondly to make a numerical simulation for each of the suggested modules and list all of the parameters. Each situation has its own set of governing equations and boundary conditions, as well as assumptions. The COMSOL Multiphysics software is a simulation application based on the COMSOL Multiphysics model. In physics, the finite element technique is used to do computations.

#### **3.2 Model Geometry Proposed**

##### **3.2.1 PV Reference (PVREF Module)**

Drawing the model geometry is the initial stage in the simulation process. PVREF module is made up of PV panels that haven't been modified in any way. Modeling as solid regions with conduction heat transfer and front glass layer, solar cells, and a rear glass layer make up convection. as indicated in Figure sheet (tedler) layer (3.1).

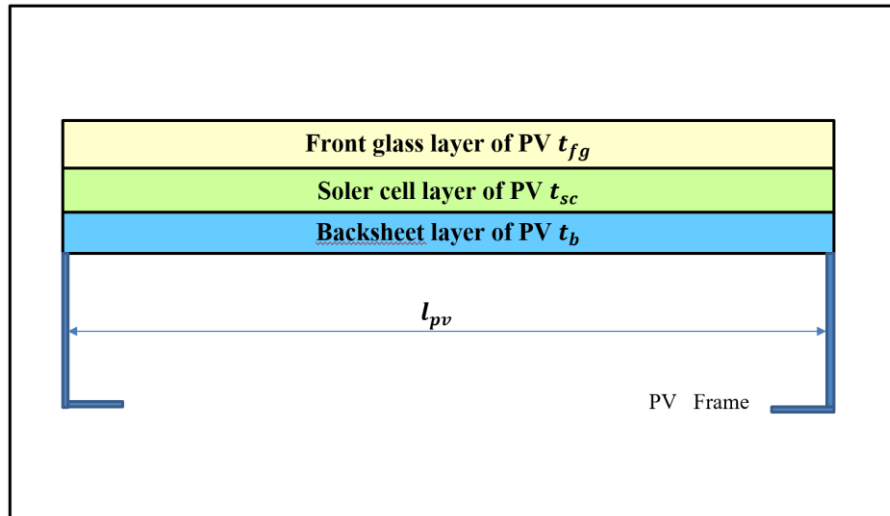


Figure (3.1) Schematic diagram of PVREF module

### 3.2.2 PV with PCM (PVT-PCM)

In the second stage of the simulation process, a phase-changing material is added, which is the bottom of the photovoltaic cell, as shown in the Figure (3.2).

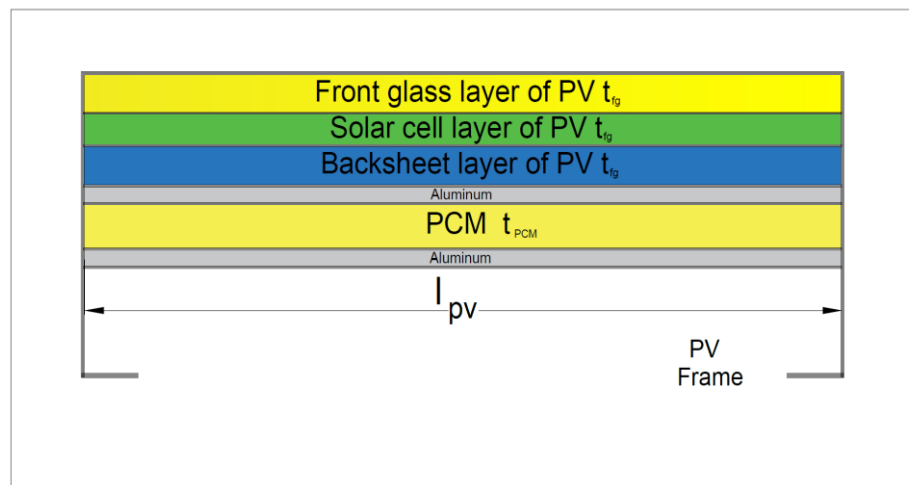


Figure (3.2) Schematic diagram of PVPCM module

### 3.3 Numerical Simulation of Proposed Modeling

The techniques for controlling the PV module temperature of operating are extremely complex. This involves internal processes that occur in the semiconductor material during the assault of photons onto the solar cell, as a result of the generation of electricity, as well as the added heat released from thermal energy derived by Photovoltaic panels as shown in table (1-3) via various Heat transmission modes, such as convection and radiation, raising the panel temperature. To test the Photovoltaic cells, the assumptions listed below regarding the hypothetical PV panel structure, the conditions of atmospheric, and other elements were made:

1. The suggested modules assumed unsteady, laminar, and 2-D flow.
2. Heat transfer coefficients are temperature-dependent.
3. Thermal losses on the sidewalls have been disregarded.
4. The characteristics of the module are changeable (temperature changes).
5. The amount of radiation emitted by the ground is insignificant.

Each module's heat balance equations can be written. Heat transmission from the module to the environment, as well as the energy received by the PCM, are used to compute the fluctuation in PV module temperature. Figure (3.3) depicts the heat transmission pathways and derived from the (PV/PCM) systems.

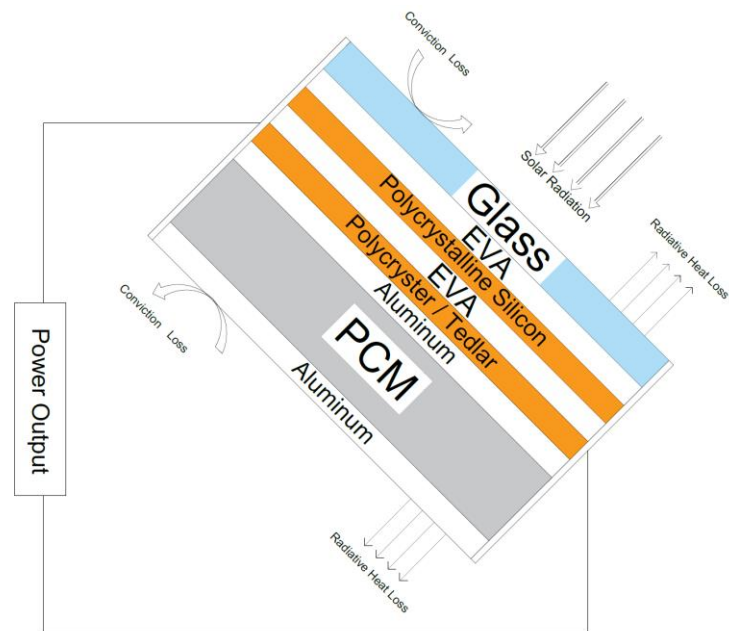


Figure (3.3) heat transmission pathways to and derived from the (PV/PCM) systems

Table (1-3) PV panel material properties [43]

PV layers	PV panel layer properties			
	Density (kg/m <sup>3</sup> )	Specific heat (Cp) (J/kgK)	Thickness (m)	Thermal conductivity (k) (W/m. K)
Face made of glass	3010	505	0.0035	1.82
EVA	961	2095	.00051	0.34
Cells of Silicon	2333	677	0.0003	150
Polyester	1210	1255	0.0005	0.22
Aluminum	2,680	900	0.005	211

Table (2-3) Thermophysical properties of PCM [44]

Properties	Value				
	SP-31	SP-50	SP-58	SP-70	SP-90
Melting Temperature ( °C)	32	50	58	71	90
Congealing area ( °C)	30	48	48	68	88
Specific heat (kJ/kgK)	210	220	250	150	150
Density (kg/L) Solid	1.35	1.4	1.4	1.5	1.7
Density (kg/L) Liquid	1.3	1.3	1.3	1.3	1.65
Thermal conductivity (W/m.K)	3 – 4	3 – 4	0.6	3 – 4	3 – 4
Max operation temperature ( °C)	50	80	85	90	110

### 3.3.1 Governing Equations

The thermal performance was simulated using the Navier-Stokes equation from computational fluid dynamics (CFD) and the following conservation equations [45].

#### 1- Conservation of Mass Equation

$$\frac{\partial \rho}{\partial t} + u \frac{\partial \rho}{\partial y} + v \frac{\partial \rho}{\partial x} + \rho \left( \frac{\partial u}{\partial x} + \frac{\partial v}{\partial y} \right) = 0 \quad (3 - 1)$$

#### 2- Conservation of Momentum Equations



In x – direction momentum equation

$$\frac{\partial u}{\partial t} + u \frac{\partial u}{\partial x} + V \frac{\partial u}{\partial y} = -\frac{1}{\rho} \frac{\partial P}{\partial x} + \nu \left( \frac{\partial^2 u}{\partial x^2} + \frac{\partial^2 u}{\partial y^2} \right) \quad (3-2)$$

In y – direction momentum equation

$$\frac{\partial v}{\partial t} + u \frac{\partial v}{\partial x} + V \frac{\partial v}{\partial y} = -\frac{1}{\rho} \frac{\partial P}{\partial y} + \nu \left( \frac{\partial^2 v}{\partial x^2} + \frac{\partial^2 v}{\partial y^2} \right) \quad (3-3)$$

### 3- Conservation of Energy Equation

$$\frac{\partial T}{\partial t} + u \frac{\partial T}{\partial x} + V \frac{\partial T}{\partial y} = \alpha \left( \frac{\partial^2 T}{\partial x^2} + \frac{\partial^2 T}{\partial y^2} \right) \quad (3-4)$$

The efficiency of the photovoltaic cells depends on module temperature. Furthermore, the performance of the PVT collectors can be depicted by a combination of the efficiency expression, comprising of thermal efficiency ( $\eta_{th}$ ) and PV efficiency ( $\eta_{el}$ ), which usually include the ratio of the useful thermal gain and electrical gain of the system to the incident solar irradiance on the collector within a specific time or period.

#### 3.3.2 PV Cell Efficiency

The PV cell conversion efficiency is not a fixed under all conditions, and it has a direct relation with the cell working temperature. The cell efficiency and produced power at a certain temperature could be calculated according to the relations (3-5) & (3-6) [46]

$$\eta_{act.} = \eta_{theo.} (1 - (0.05(T_c - 25))) \quad (3-5)$$

$$P = P_{sad} (\eta_{act} / \eta_{theo}) \quad (3-6)$$

$\eta_{act}$  is the actual efficiency,  $\eta_{theo}$  is the standard efficiency of the PV module,  $T_c$  is the temperature of the solar cells ( $^{\circ}\text{C}$ ), and  $P$  is the power,  $P_{sad}$  is power standard.

### 3.4 The CFD model

The thermal performance of the PV panel with PCM cooling was calculated using a numerical study. COMSOL Multiphysics 5.5 software was used to create the computer simulation, which was based on computational fluid dynamics (CFD) finite element computations.

#### 3.4.1 Computational Fluid Dynamics software COMSOL Multiphysics

CFD issues are extremely nonlinear and need the use of high-precision finite element software to solve. Because CFD software are capable of computing fluid dynamics, they will be used to calculate:

1. The thermal behavior of PV panels with PCM cooling
2. The total amount of time it takes to attain the steady-state condition.
3. Heat distribution in conjunction with the photovoltaic panel
4. Temperature of the output

#### 3.4.2 Model Geometry

The right case geometry architecture, to be solved, is the initial stage in computing the best outcomes. In this situation, as shown in Figure (3.5), the geometry was produced using the same program. All of the original

module's pieces are included in the geometry, along with the identical material characteristics.

### **3.4.3 Use of COMSOL Multiphysics Mesh independency check**

COMSOL Multiphysics 5.5 software is used to solve highly complex problems based on the finite element method. Furthermore, the CFD model must be derived into smaller forms of elements for a mathematical solution to solve for heat transfer. In this case, the network was created by COMSOL Multiphysics 5.5 itself with a total of elements 14590. In order to obtain the exact number of mesh facets for a proper computation Figure (3.4), mesh independence has been proposed in this study to ensure the maximum possible accuracy Figure (3.5). The test helps us determine the correct number of faces. In this study, the tested mesh faces 9121, 9526, 10860, 12205, 14590, 17890 were used to calculate the average cell temperature. The first four options give a slight variation in the results. However, the results start converging after 14590 elements as shown in Figure (3.6) Therefore, the grid containing 14590 elements were chosen to calculate the average cell temperature.

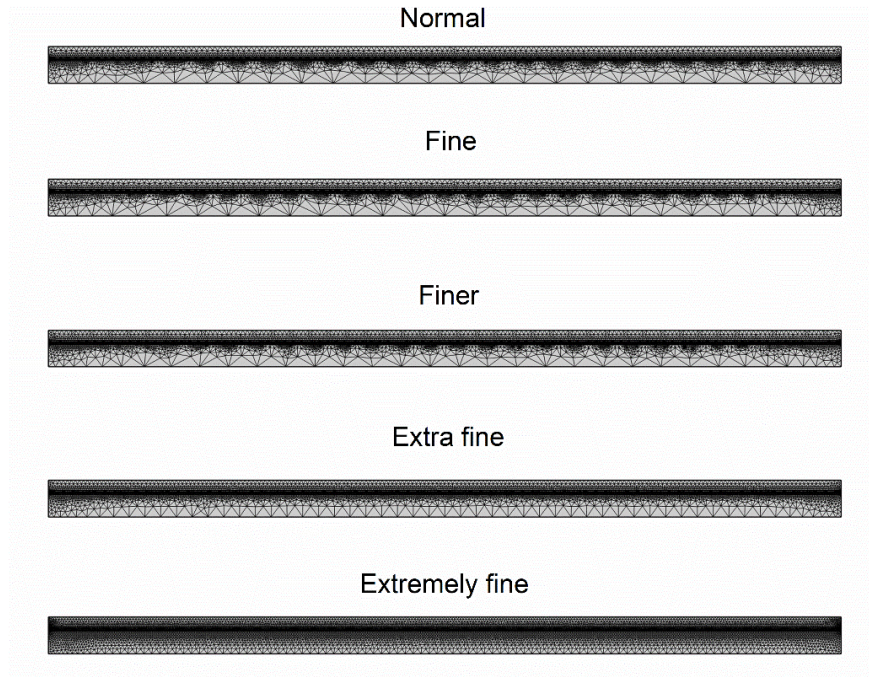


Figure (3.4) Different types of meshing for PV module

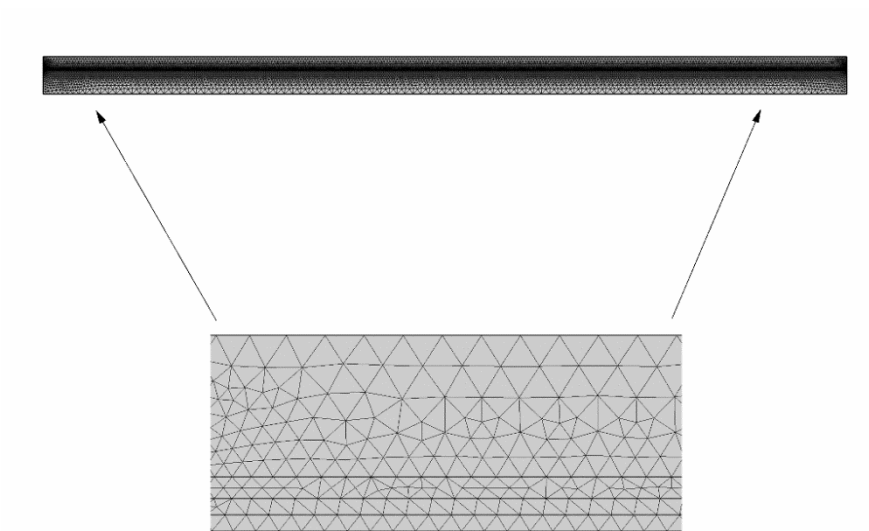


Figure (3.5) Mesh at a mid-height cross section of the numerical model.

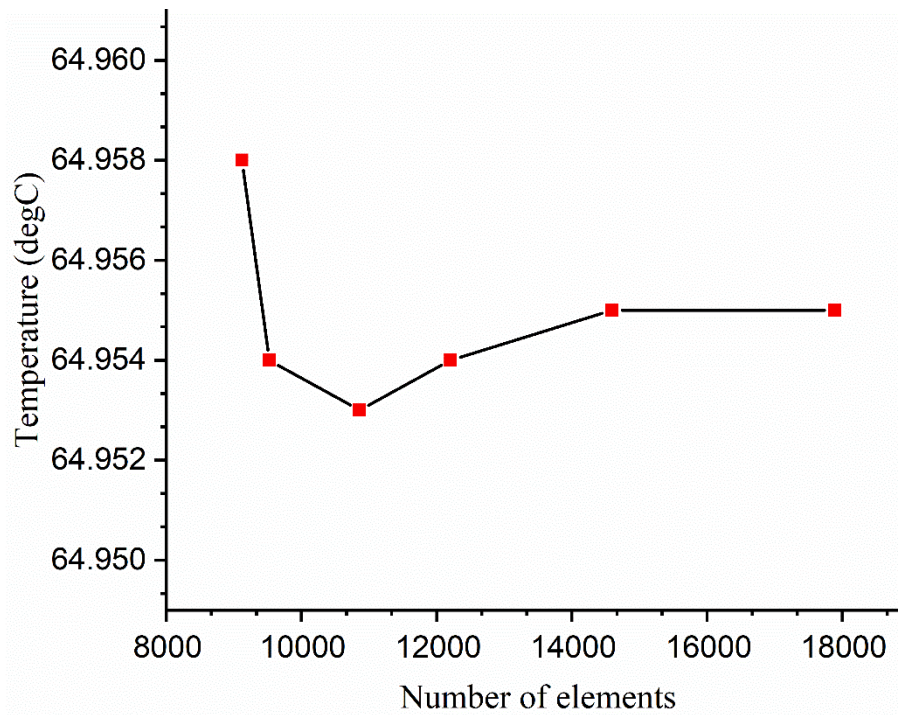


Figure (3.6) Mesh stability test

### 3-5 Code Validation

The validity of the current 2D simulation is difficult to find a comparable study for comparison, so the validity was only established for PVREF. The current model for PVREF was carried out and a comparison with numerical simulation findings of Table (3-3). Angham Fadil et al. [25] The experimental work of the two-dimensional photovoltaic panel, which is based on readings for the same time zone, provided a great convergence with temperatures that reached 7% Figure (3.7).

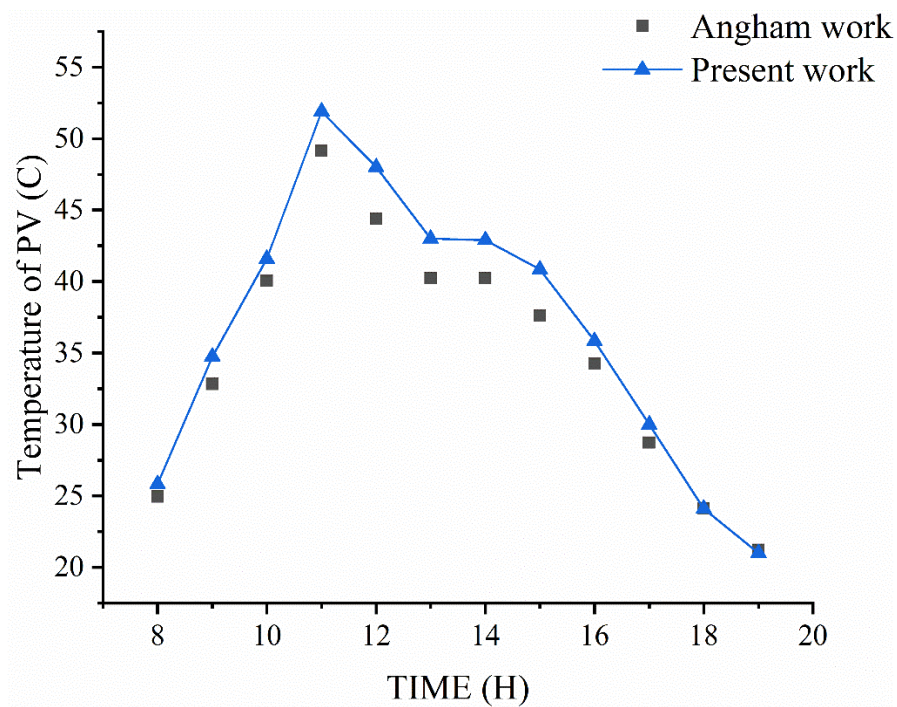


Figure (3.7) The simulated results of solar cells temperatures during the test day for PVREF.

Table (3-3) Code Validation

Validation design parameters	Value (Angham)	Value (Percent work)
The length of the PV module, $l_{pv}$	0.539 m	0.2 m
The width of the PV module, $W_{pv}$	0.66 m	0.13 m
The module area, $A_m$	$0.539 \times 0.66 \text{ m}^2$	$0.2 \times 0.13 \text{ m}^2$
The thickness of front glass cover, $t_{fg}$	0.0032 m	0.0032 m
The heat conductivity of front glass cover, $K_{fg}$	1 W/m K	1 W/m K

The absorptivity of glass cover, $\alpha_{fg}$	0.06	0.06
The transmissivity of glass cover, $\tau_{fg}$	0.84	0.84
The emissivity of glass cover, $\epsilon_{fg}$	0.93	0.93
The thickness of solar cell, $t_{sc}$	0.0003 m	0.0003 m
The absorptivity of solar cell, $\alpha_{sc}$	0.85	0.85
The heat conductivity of solar cell, $K_{sc}$	0.036 W/m K	0.036 W/m K
The thickness of back sheet, $t_b$	0.0005 m	0.0005 m
The heat conductivity of back sheet, $K_b$	0.033 W/m K	0.033 W/m K
The absorptivity of back sheet, $\alpha_b$	0.8	0.8
The packing factor, $\beta$	0.88	0.88
The temperature coefficient, $\beta_p$	0.0045	0.0045
The thermal power conversion factor, $C_f$	0.3	0.3

## Chapter Four

### Experimental Work

#### 4-1 Introduction

This chapter will focus on the process of connecting cells, as well as realistic methods for monitoring cell voltage and measurement equipment's, will be explored. This research was conducted on the rooftop of a building in Najaf, Iraq, at [(32.1°] N latitude and [44.19°] E longitude, in a demanding climate that causes solar panel efficiency to decline during hot seasons.

#### 4-2 System components

The working fluid in this system is a phase change material whose purpose is to cool the solar cell and conserve energy in order to benefit from it at sunset (at night). The system consists of three solar cells, thermal sensor, and phase-changer material that are held together on a frame as shown in the Figure (4.1). it can also be seen a practical picture of a device at the work site, could be seen as in the Figure (4.2).



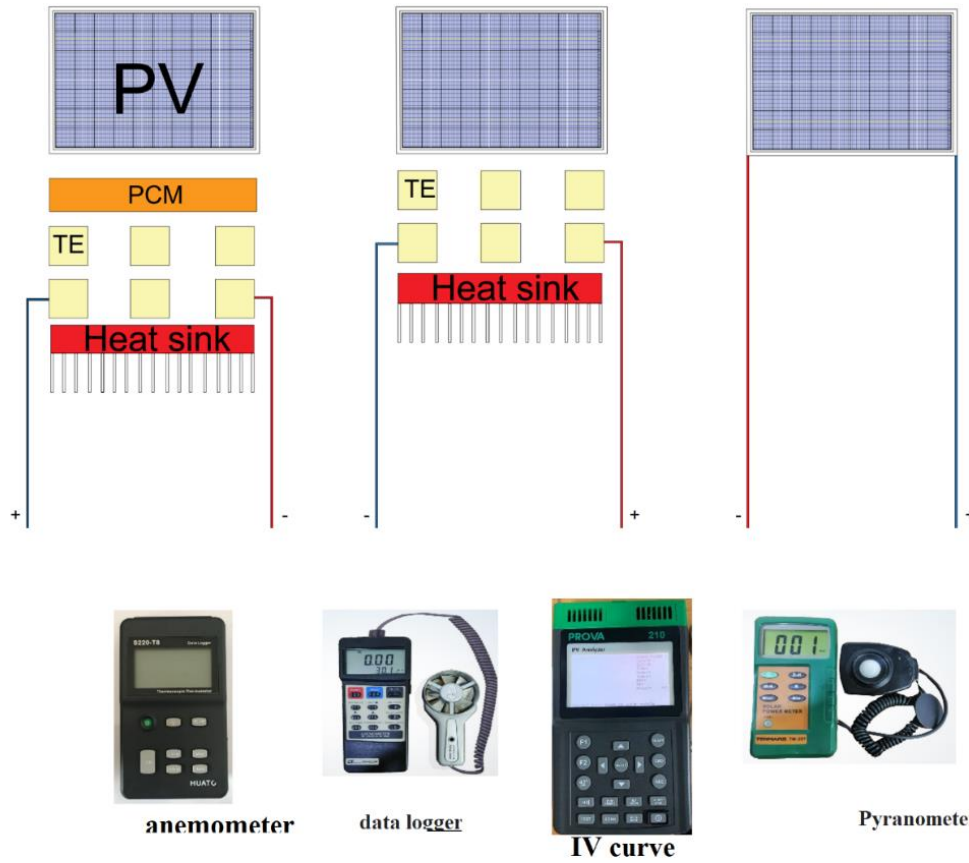


Figure (4.1) Schematic diagram of the PV module cooling system with its all parts

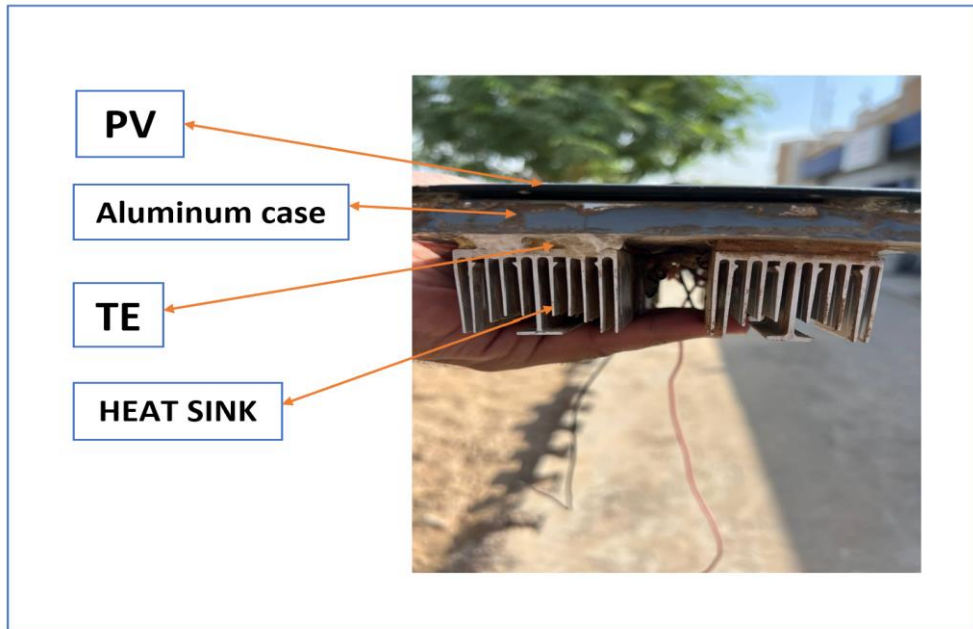


Figure (4.2) The device while working during the day

### 4-2-1 The photovoltaic panel

The photovoltaic panel is the most important component of any solar system, and the solar panels employed in this study are polycrystalline panels with three layers (glass, EVA, and back sheet). The photovoltaic panel is mounted on the roof. The city of Najaf / Iraq is located at [(32.1°] N latitude and [44.19°] E longitude in the direction of at a 31.5-degree angle to the south the plate specs were as table(4-1).



Figure (4.3) Photovoltaic module

Table (4.1) Photovoltaic specifications

<b>NO</b>	<b>Item</b>	<b>Description</b>
1	Model type	UrukTECK
2	Solar cell type	Polycrystalline silicon
3	Size (mm)	200*130*2.5
4	Maximum power	4.2 W
5	Voltage at Pmax. (V)	18
6	Current at Pmax. (A)	0.22

7	Open circuit voltage (V)	21.5
9	Weight (Kg)	0.088
10	Efficiency (%)	15- 17
11	Standard test condition	1000 w/ m <sup>2</sup> , 25 °C
12	Operation Temperature	-40 °C TO +85 °C

#### 4-2-2- Thermal Electric Device

A thermoelectric generator (TEG), also called a Seebeck generator, is a device that converts thermal energy (temperature differences) directly into electrical energy through a phenomenon called the Seebeck effect. The model used is shown in the Table (4-2):

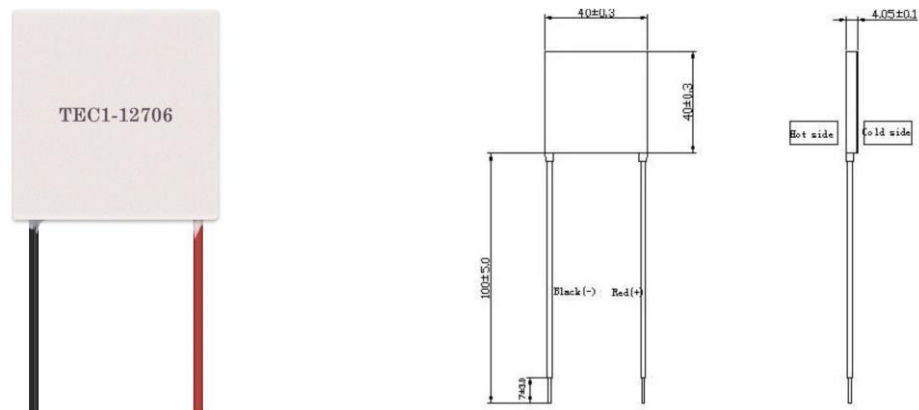


Figure (4.4) Thermal electric module

Table (4.2) Thermal electric specifications

Name	TEC1-12706
------	------------

Dim.	40*40*4.05 mm
Feature	Lightweight and small
$I_{\max}$	6 A
$V_{\max}$	15.4 V
$Q_{\max}$	53 W

### 4-3 Heat sink

The heat sink is designed to increase the heat exchange surface (made of aluminum) and the heat sink is installed by thermal paste. The paste improves the energy of the heat sink by filling the air column between the heat sink and the heat distributor of the device Figure 4.5.

Table (4.3) Heat sink specifications

Dim.	40 * 40 * 40mm
Num.Fins	30
Feature	lightweight and Small
Metal	Aluminum
Density	2680 (kg/m <sup>3</sup> )
Thermal conductivity	211 (W/m. K)
Specific heat capacity	900 (J/kg. K)
Emissivity	0.67



Figure (4.5) Heat sink module

#### **4-2-4 Aluminum Container**

For the purpose of installing the PCM material, a container made of aluminum with dimensions (130 \* 200) mm is used, which is installed beneath the solar cell, as shown in Figure (4.6). Aluminum was chosen for its high conductivity, reaching up to.

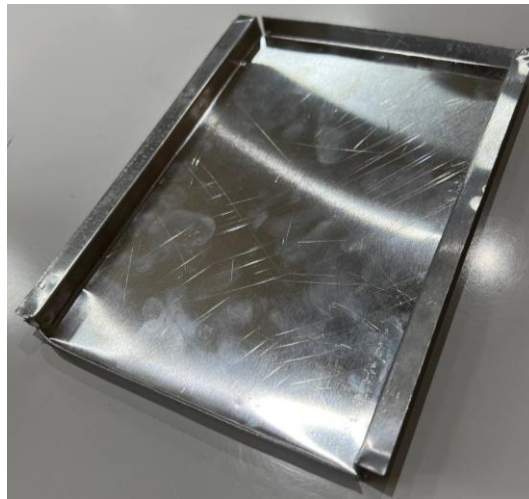


Figure (4.6) aluminum container

#### 4-2-5 PCM Preparation

The German-made SP-31 wax was used, and it can keep high temperatures up to 50 °C. The PCM preparations are shown in Appendix A.



Figure (4.7) PCM Precision Parts

#### 4-2-6 Thermal Preparation

Thermal Grease Paste aids thermal conductivity and heat dissipation in electrical appliances, ensuring the stability of electronic instruments, meters, and other electrical devices.

Specification		
1	Model	HY510
2	Thermal Conductivity	>1.93 W/m-K
3	Thermal Resistance	<0.225° C-in <sup>2</sup> /W
4	Color	Grey
5	Net Weight	30g



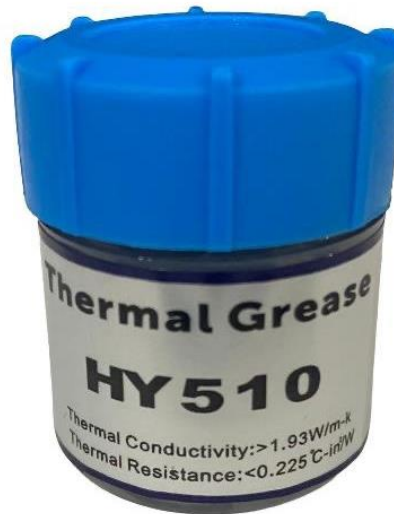


Figure (4.8) Thermal Grease Paste

### 4-3 Measurements

The model was designed to be tiny in order to facilitate portability and movement. The gadget is placed in Najaf Engineering Technical College. During the month of May. Four types of specific measuring equipment are employed in these tests, and they are classed according to their distinct roles as follows :

#### 4-3-1 Thermocouple

Temperature measurements are taken at various sites within and outside the sun using k-type thermocouples with a reading accuracy of 0.2 percent  $1^{\circ}\text{C}$ . It features eight calibrated thermocouples with 0.75 mm probes spaced on the inner and outer cover, the TE, the PCM enclosure, and the perimeter. As indicated in the diagram, they are all connected to the number 8 channel type screen thermometer (Figure 4.9).





Figure (4.9) Thermocouples and data logger

#### 4-3-2 pyranometer

A device (solar power meter) measuring the intensity of solar radiation was used to measure direct solar radiation per hour in the direction of PVT. As illustrated in Figure (4.10), this device type TENMARS (TM-207) model has an accuracy of  $(\pm 5\%, \pm 10 \text{ W /m}^2)$  .



Figure (4.9) Solar radiation measurement device (Pyranometer)

#### 4-3-3 Anemometer

Every hour, the wind speed was measured to see how it influenced the PVT productivity. An anemometer gadget is used to take hourly readings. This

device parameters, type (AM-4206M), range (0.4 - 30m/s), accuracy (1.8 percent N+2d), and illustration is shown in Figure (4.11).

In addition to the findings received from the weather station, which is placed at 10 m above ground, a pyranometer and anemometer were employed. An Iraq's Najaf Engineering Technical College, this station monitors solar radiation in ( $\text{W}/\text{m}^2$ ) units, with a range of 0 to  $1800 \text{ W}/\text{m}^2$  and an accuracy of  $\pm 0.3\%$ .



Figure (4.11) Air flow meter device (anemometer)

#### 4-3-4 PV Module Analyzer

As shown in Figure (4.12), we used the solar module analyzer type PROVA200A. 13). This system is one of the main equipment used in the specification investigation of the PV module, for the PV module to read the maximum value ( $P_{\text{max}}$ ) of photovoltaic power generation and display the maximum estimated voltage ( $V_{\text{max}}$ ). Displays the (I-V) and (P-V) curves. Maximum current ( $I_{\text{max}}$ ), open circuit voltage (V), short circuit current (I),

and electrical efficiency estimation. Application Software Type 6 AV131029 Solar panel analyzer and USB.

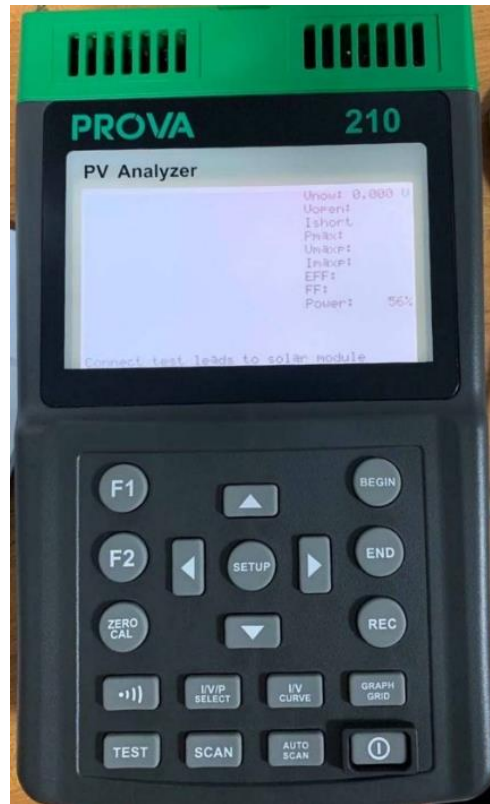


Figure (4-12) PROVA 200A Solar module analyzer

#### 4-4 Process of conducting the experiment

After completing the assembly of the parts of the model, the measuring equipment and tools are connected to the model, which are:

- 1- The thermocouple: the temperatures are measured in four locations where a fixed thermocouple is installed that measures the ambient temperature and distributes the other three to the models that are only PV model, (PV + TE) model and (PV+PCM+TE) model where they are installed below each model, calibration was performed between

the thermocouples used and the mercury thermometer in Appendix B.

- 2- Solar radiation intensity sensor is placed and installed in the frame to install the hourly direct solar radiation reading and it has been calibrated in Annex (C).
- 3- Wind Speed Sensor is installed on the frame for the purpose of measuring the local wind speed hourly and the device is calibrated in Annex (D).
- 4- IV Carve device Solar cell connections are installed in the device and connected to the computer for the readings for the purpose of displaying the efficiency and electrical capacity every hour.

All measuring devices are operated during the measurement period from 0 to 24 o'clock for a whole day, which is on 13-5-2022. All data were recorded manually and for every hour, where experiments were conducted on the highest surface in the city of Najaf.

## **Chapter Five**

### **Results and Discussion**

#### **5.1 General**

This chapter will examine the process of connecting cells, as well as practical ways for monitoring cell voltage and measuring equipment.

This study was carried out on the rooftop of a building in Najaf, Iraq, at [(32.1°] N latitude and [44.19°] E longitude, in a challenging climate that causes solar panel efficiency to decrease during hot seasons. All theoretical results studied were in May 2022.

#### **5.2 Numerical results**

##### **5-2-1 Verification Model**

The characteristics of the photovoltaic cooling system were simulated, and the optimal was selected, which gives the best results using the simulation by COMSOL 5.5 software to reduce the temperature of the photovoltaic base, and then increase its efficiency and performance in proportion to the weather conditions in the region.

##### **5-2-2 Surrounding conditions and work site**

This study relied on the coordinates of the city of Najaf / Iraq, the readings of atmospheric conditions were taken from the center of the weather forecast at the Technical College of Engineering Najaf for the day 13-5-2022 and were shown in Figure (5.1) (A, B, C), which included the intensity of solar radiation, air temperature and wind speed .

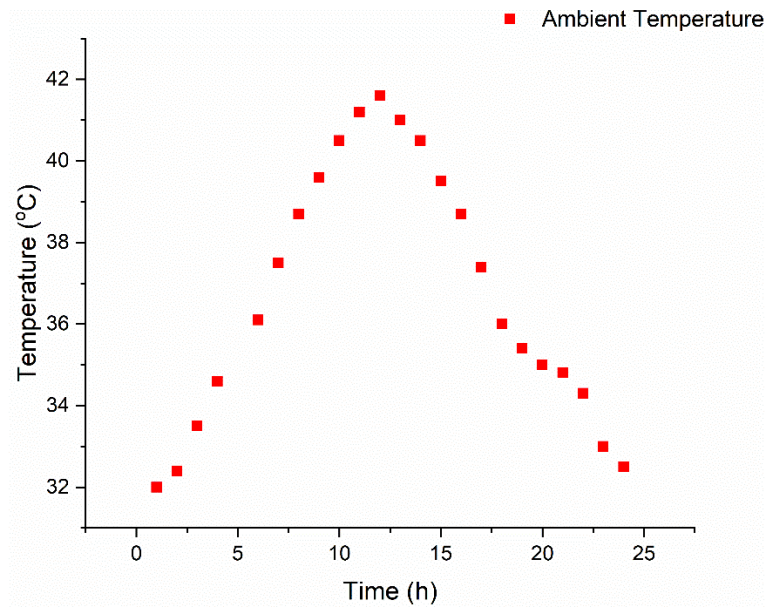


Figure (5.1) A Temperature change over time

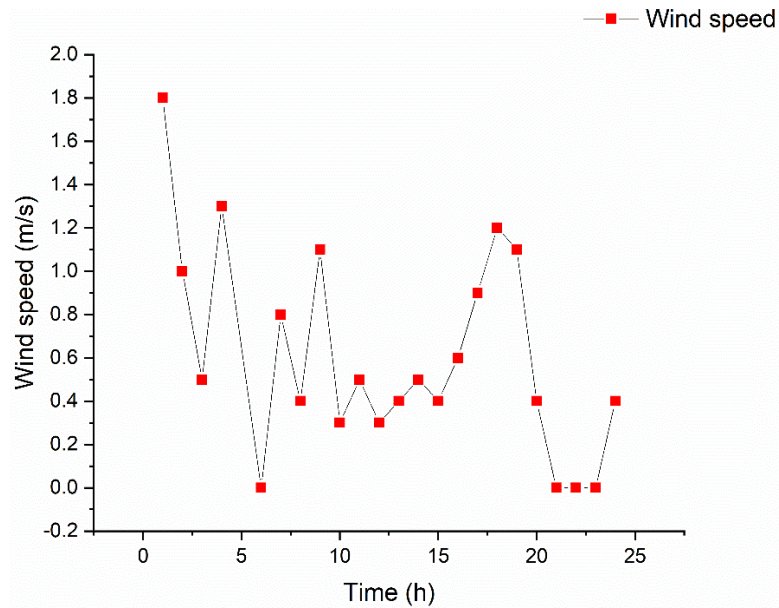


Figure (5.1) B. Wind Speed over time

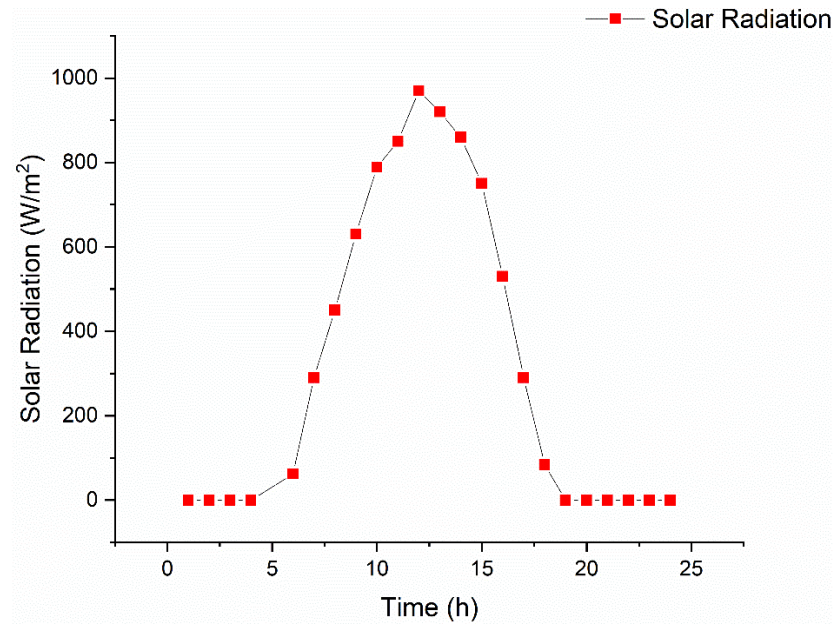


Figure (5.1) C. Solar radiation over time

### 5-2-3 Effect of PCM mass

Figure (5.2) A,B shows the results of testing different quantities of PCM, as it appears from the figure that the amount of heat coming from the sun is sufficient to dissolve PCM completely by 200 g according to the dimensions, as all the amount melted at 1 pm where everything was the lower PCM depth, the faster the melting, the results indicate that the temperature of the solar cell reaches its maximum at about 1 pm as solar radiation will reach the maximum and the process of solidification of the phase-changing material takes more time after sunset, which is required for heat storage.



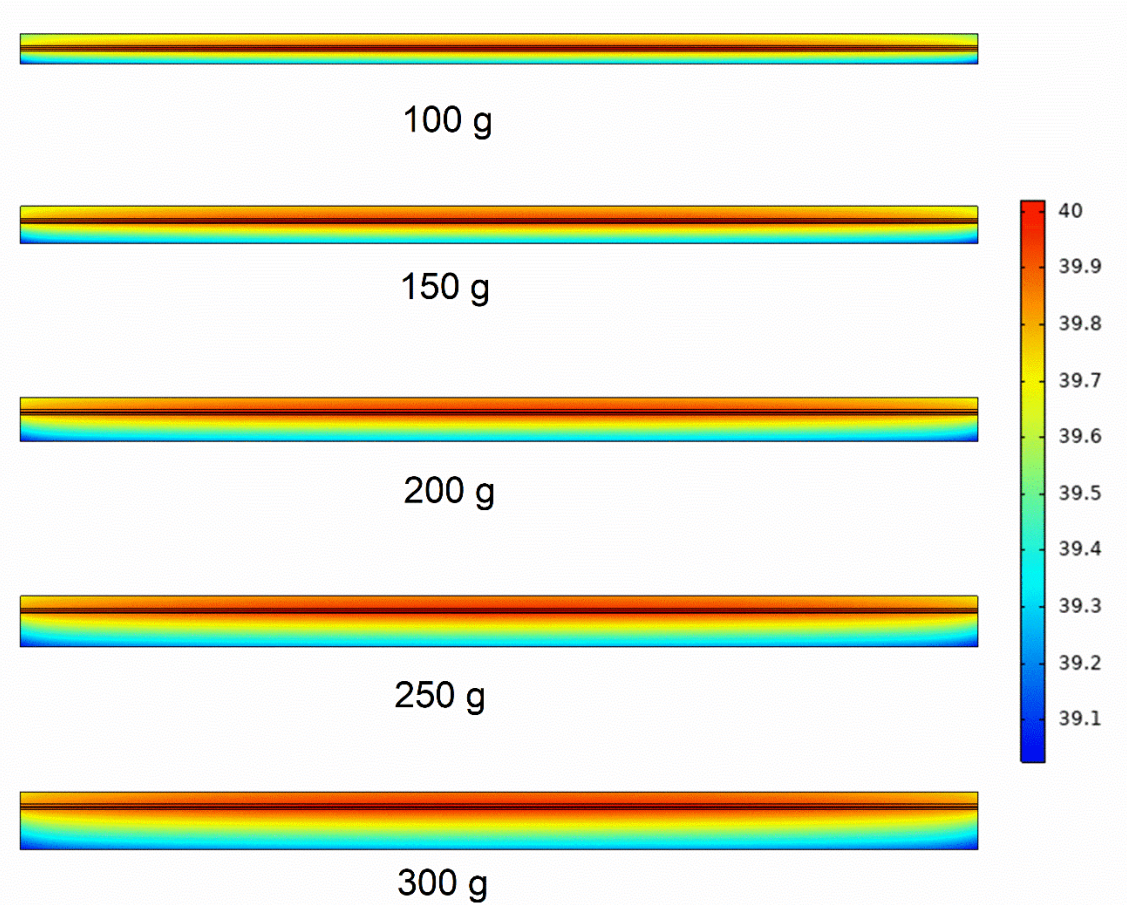


Figure (5.2) A- Effect of PCM (SP-31) mass



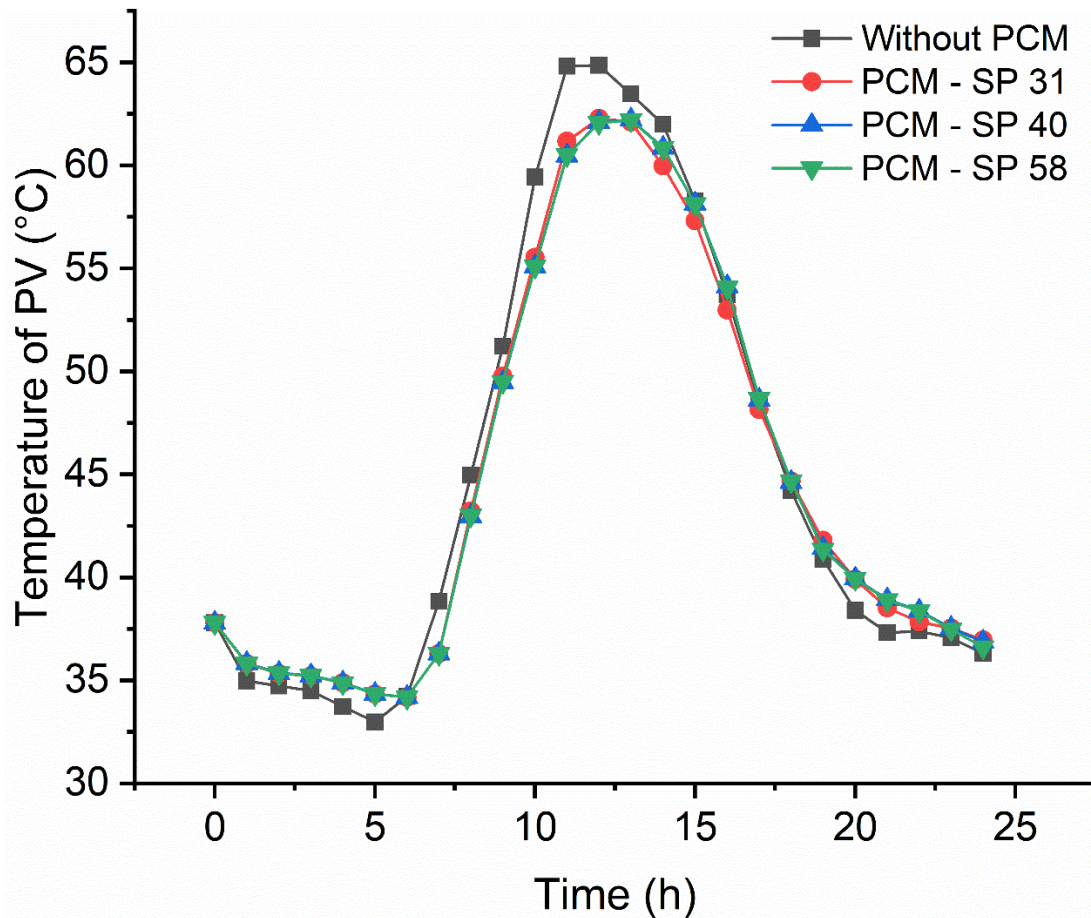


Figure (5.2) B- The relationship between temperature of PV and type of PCM

#### 5-2-4 Change State of The PCM Material from Solid to Liquid with Time

The beginning of the experiment is from 0:00 to 6:00 At. The material remains in the solid state because there is no solar radiation during this time of the day. In the daytime, temperatures start to rise. When the temperature of the solid PCM reaches the transition point, the energy is stored as latent heat, as seen in Figure (5.3). The melting process improves with time, and it accelerates when the PCM in liquid phase comes into contact with the back

of the aluminum plate. Melting occurs between 8:00 a.m. and 5:00 p.m., which is warmer than the PCM melt temperature.

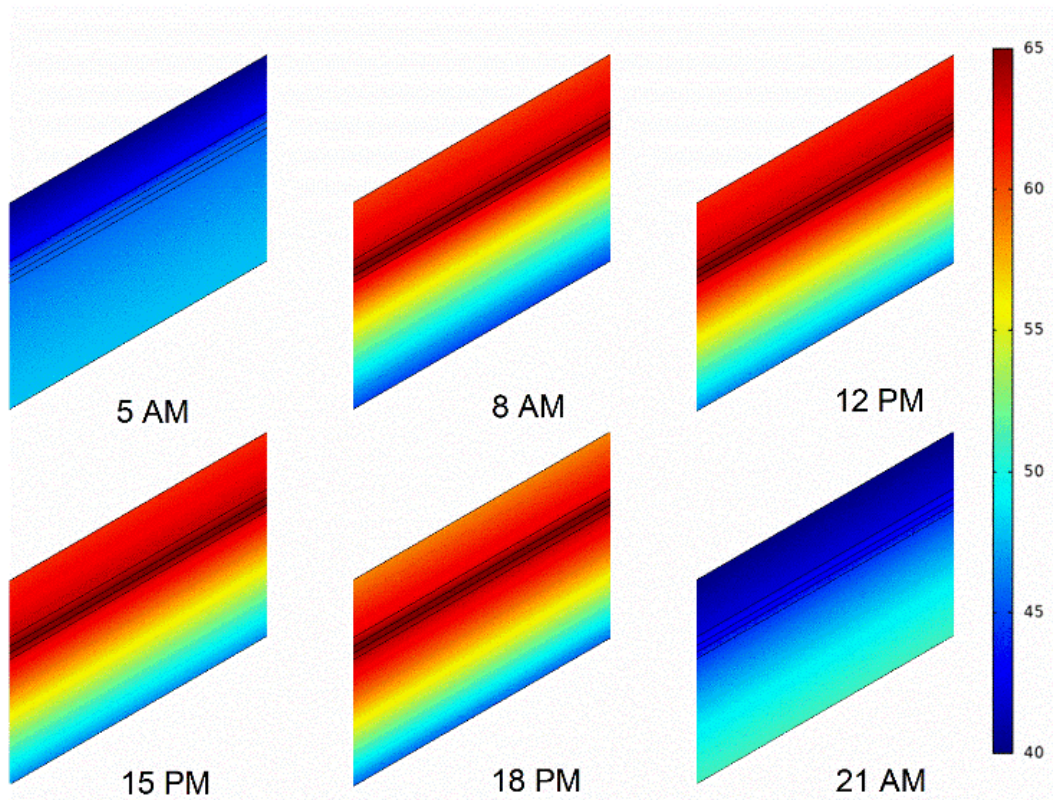


Figure (5.3) Stages of transformation of the PCM during the day

The PCM begins to harden at 06:00 p.m. and is fully formed by 08:00 p.m. It's worth noting that during solidification, the PCM's velocity produced by natural convection is approximately zero, indicating that conduction heat transfer takes precedence. Figure (5.3) depicts the fluctuation in PCM melt fraction over the course of a day. It demonstrates that solidification processes are completed in roughly 2 hours.

### 5-2-5 Power output and efficiency

The temperature of the photovoltaic panel affects the power, as shown in Figure (5.4). The use of PCM is intended to regulate the temperature of the photovoltaic module. We can see a significant decrease in power loss, and this does not happen because of the high temperature, but rather because of the phase change, where the PCM delays the rise in temperature by absorbing the additional thermal energy of the system, and convection plays a role in increasing the heat transfer with the surrounding environment. The maximum output power is 290W with no PCM and 305W is reported as PCM behind the photovoltaic panel Figure (5.4). As for the efficiency of the photovoltaic panel, it is inversely proportional to the increase in temperature. Therefore, the efficiency increases in the presence of the phase-changing material, where it reaches 14 % at Figure (5.5), noting that the ambient temperature is very high, up to 42 °C.

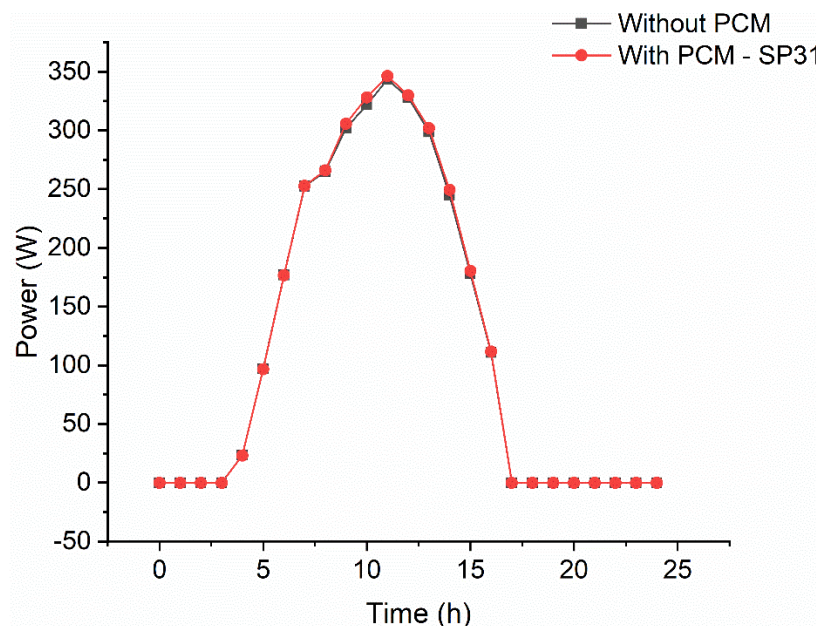


Figure (5.4) Variation of power with and without PCM.



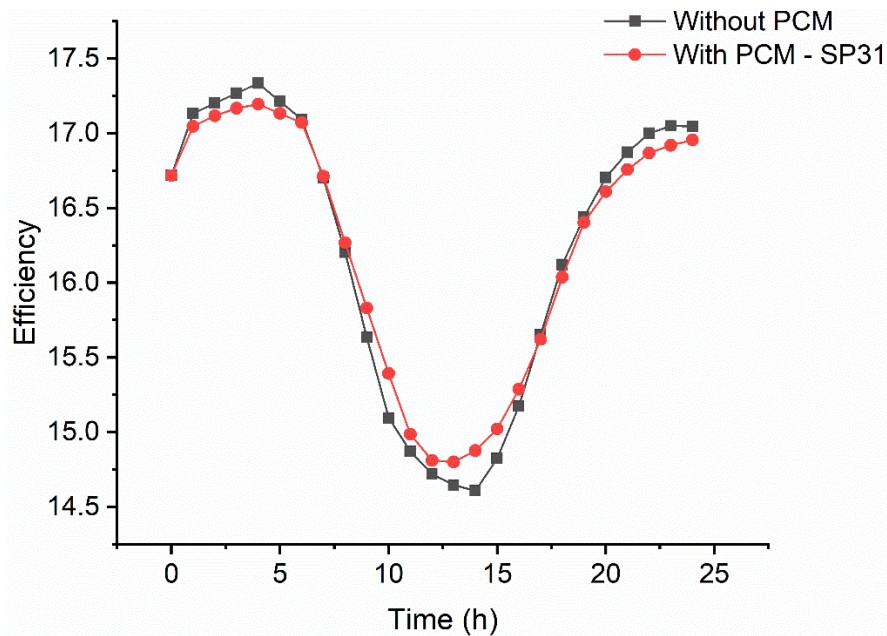


Figure (5.5) Variation of efficiency with and without PCM.

### 5.3 Experimental results

Experimental results were obtained using the described PV module with an area  $0.026 \text{ m}^2$  and standard conversion efficiency of 17 % compared to a PV panel operating at the same time with the same specifications. To obtain the best results, three cases are selected to study only the first PV, second PV-TE and third PV-PCM-TE cases. Each experiment will focus on several variables, the most important of which are.

- 1- Thermal behavior of the surfaces of photovoltaic panels during the cooling period.
- 2- Photoelectric behavior and cell efficiency according to low temperature.
- 3- Total energy produced for the photovoltaic panel with and without PCM cooling.

4- Total energy produced by TE during the day and at night.

The experiment was conducted on the 13 of May 2022 at 0:00 AM to 23:59 PM. The maximum solar radiation recorded was  $990 \text{ W/m}^2$  while the maximum ambient temperature and average wind speed recorded was  $42^\circ\text{C}$  and  $1.2 \text{ m/s}$ , respectively.

### 5.3.1 Atmospheric Conditions Practically Measured By Measuring Instruments

As was already noted, solar radiation directly affects the temperature of the cell. The solar radiation varies in the current work as depicted in Figure (5-6). Wind speed and outside temperature are two significant parameters that affect the temperature of the PV cells. Convection heat transfer from the PV module surface and its base is affected by the wind speed during end hours, as shown in Figure (5-7). The change in ambient temperature during the day is depicted in Figure (5-8).

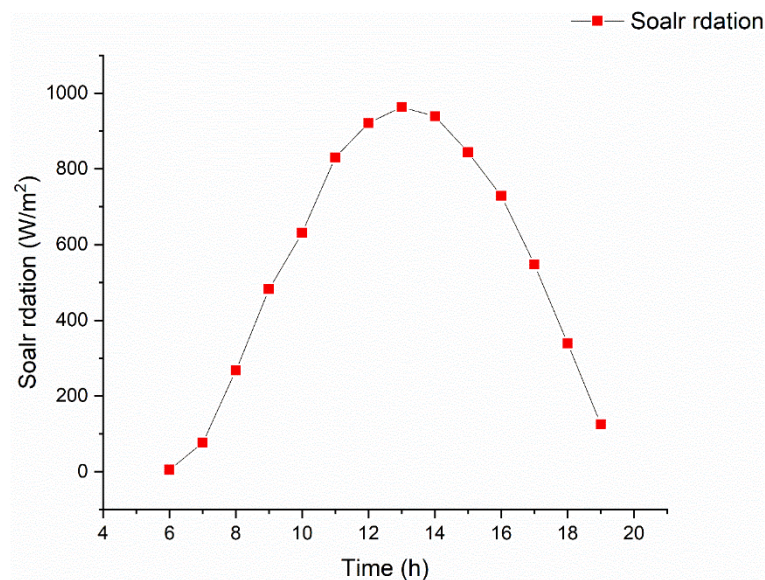


Figure (5.6) Solar radiation changes during daylight hours.

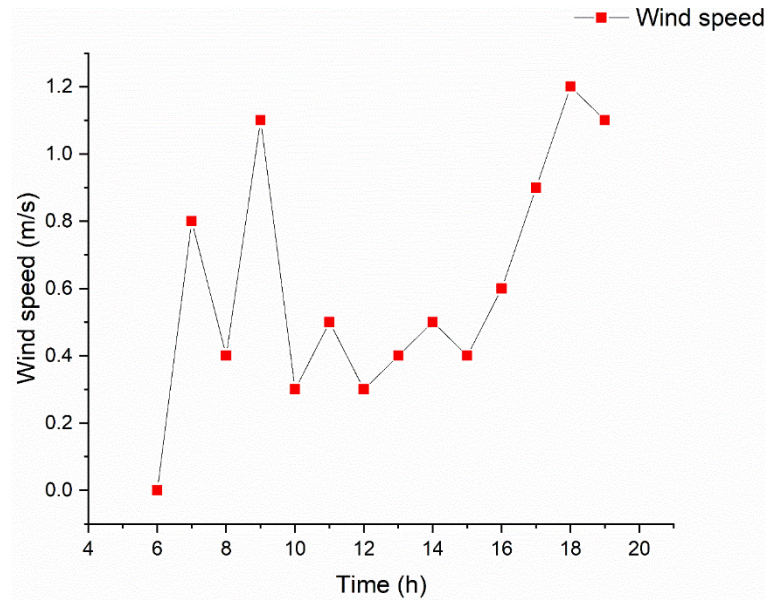


Figure (5.7) Wind speed changes during daylight hours

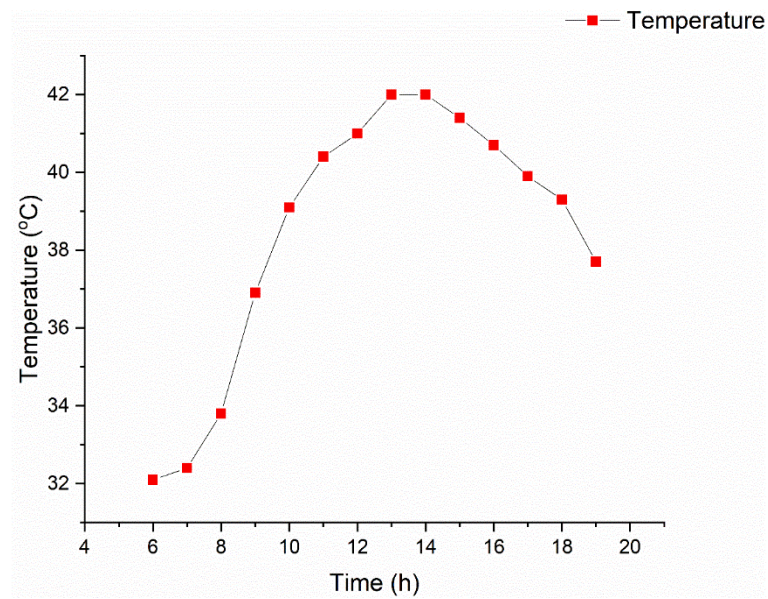


Figure (5.8) Ambient temperature changes during daylight hours.

### 5-3-2 Effect of Adding a Phase Change Material on the Temperature

It is known that the photovoltaic unit converts a small part of the falling solar rays into electrical energy, and the remaining part turns into thermal energy. The energy increases the temperature of the cell, reaching approximately 54 °C. In Figure (5.9), it can be noticed the effect of adding Thermal Electric device behind the solar cell, where the temperature decreased by a degree one °C and 2.5 °C for the cell containing PCM, note that the maximum air temperature was 42 °C in the experiment. It is noted from the curves of temperature that the temperature difference between the solar cell and the ambient temperature is approximately 14°C at the time of peak and this difference increases the generation of electricity by Thermal electric device.

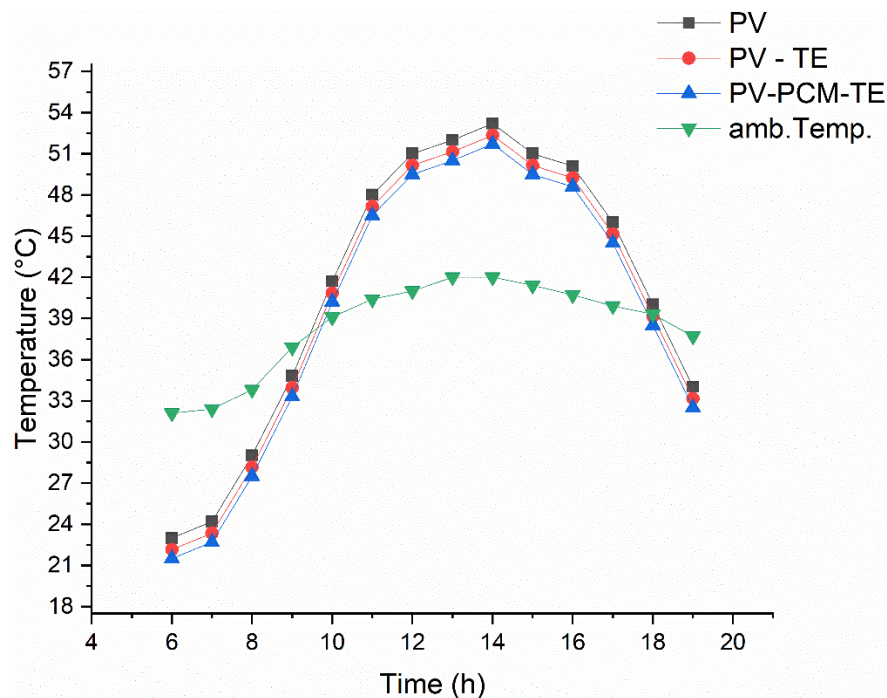


Figure (5.9) shows the Temp. of the three models and ambient Temp.



### 5-3-3 Effect of adding phase change material on the efficiency

The efficiency of the photovoltaic cell is closely related to the working temperature in Figure (5.10) Experimental measurements of the three models show that the efficiency begins to decrease with increasing temperature. It is noted that the model that contains a phase-changing material has the highest efficiency by a small difference, due to the smallness of the model used, where the efficiency of 14.58, 14.65, 14.72 % was recorded, respectively.

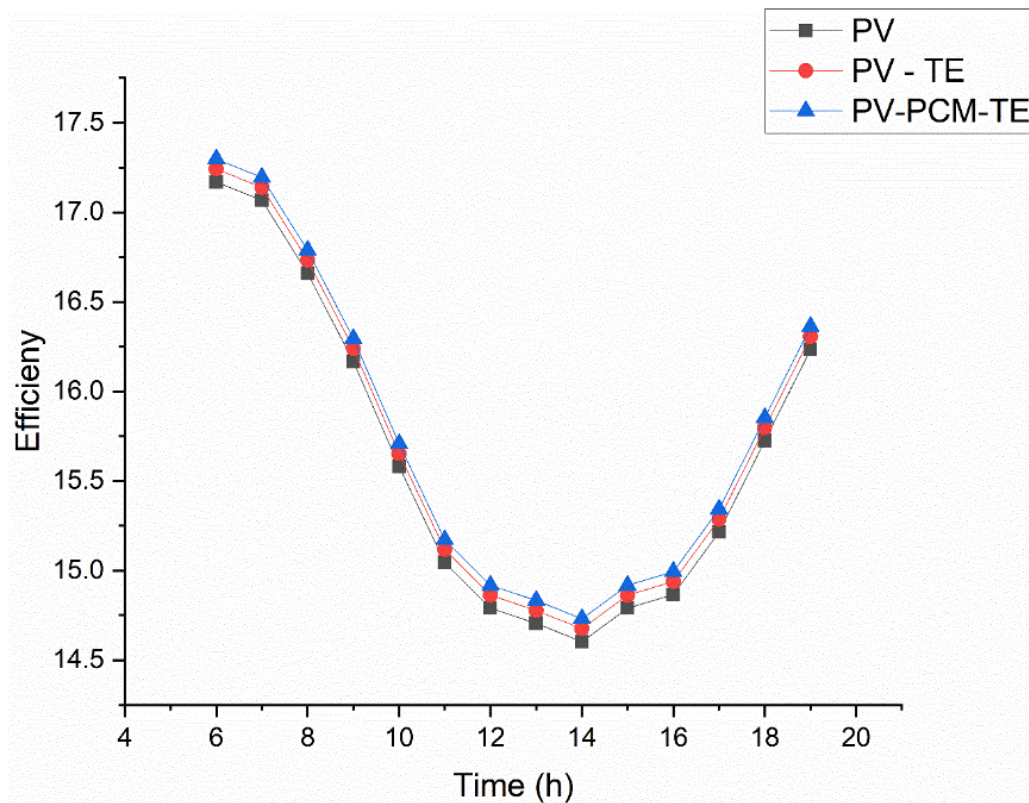


Figure (5.10) Effect of adding phase change material on the efficiency



#### **5-3-4 Effect of adding phase change material on the power**

As the efficiency of the cell increases, the total power produced by the photovoltaic panel increases. Figure (5.11) shows the amount of increase in the power produced, as the model that contains a phase changing material had a little higher power at the peak time. By observing the curves, it can be noticed that when the temperature starts to rise from 8 in the morning until the phase-changing substance melts at 10:30 in the morning, the effect of the substance on the power curve can be clearly seen and then it settles. As shown in the figure:

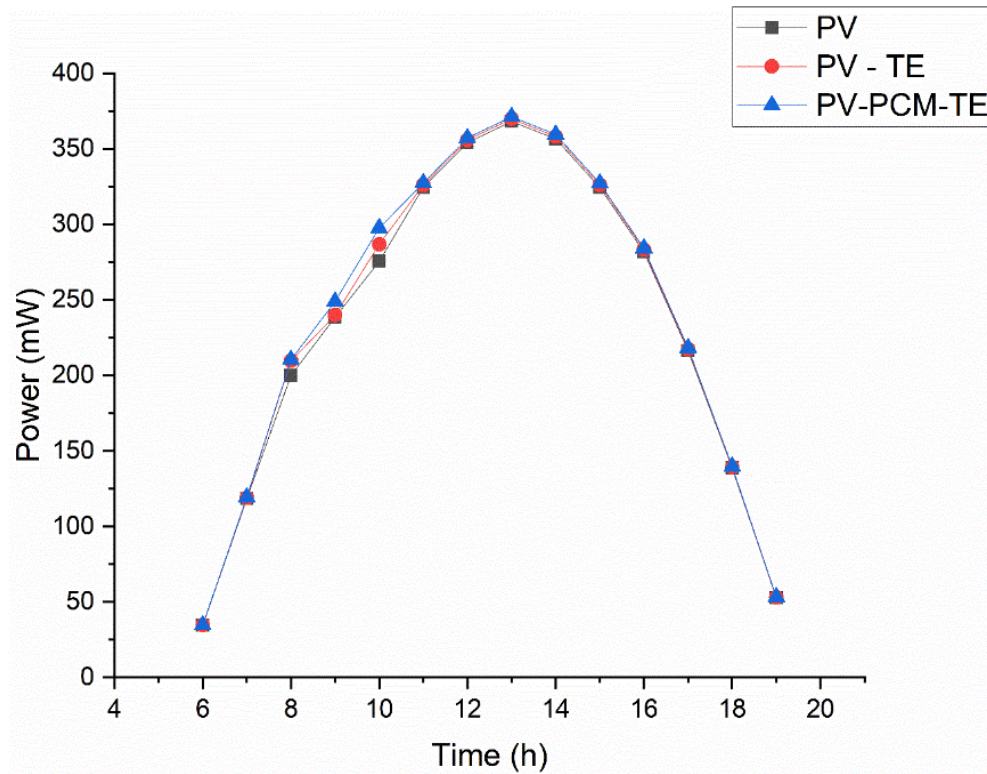


Figure (5.11) Effect of adding phase change material on the power

### 5-3-5 The effect of adding TE to generate electricity at night

The test results showed that the proposed outdoor can generate electricity during the day and at night continuously without dropping to zero.

In Figure (5-12), there are two curves, the first black representing (PV-TE) for six TE devices and for a period of 24 hours, the curve begins to rise from 6:00 AM at sunrise to reach its highest level at (10:00) AM, the curve starts declining because it is affected by atmospheric temperatures and wind speed, as shown in the Figure (5.7) (5.8). The red curve represents the voltage generated by TE also for six devices, but with the addition of a phase-changing material between TE and PV, where we notice a decrease in the curve at 10:00 AM because it is affected by wind and temperatures and

it began to rise from 12:00 AM again after melting PCM and turning it into a liquid, we notice after sunset that the heat content of PCM remains high and TE continues to generate electricity until night. The rate of electricity generation during the day was 62,42 mV and at a rate of 10.1 and 6.8 mV at night respectively.

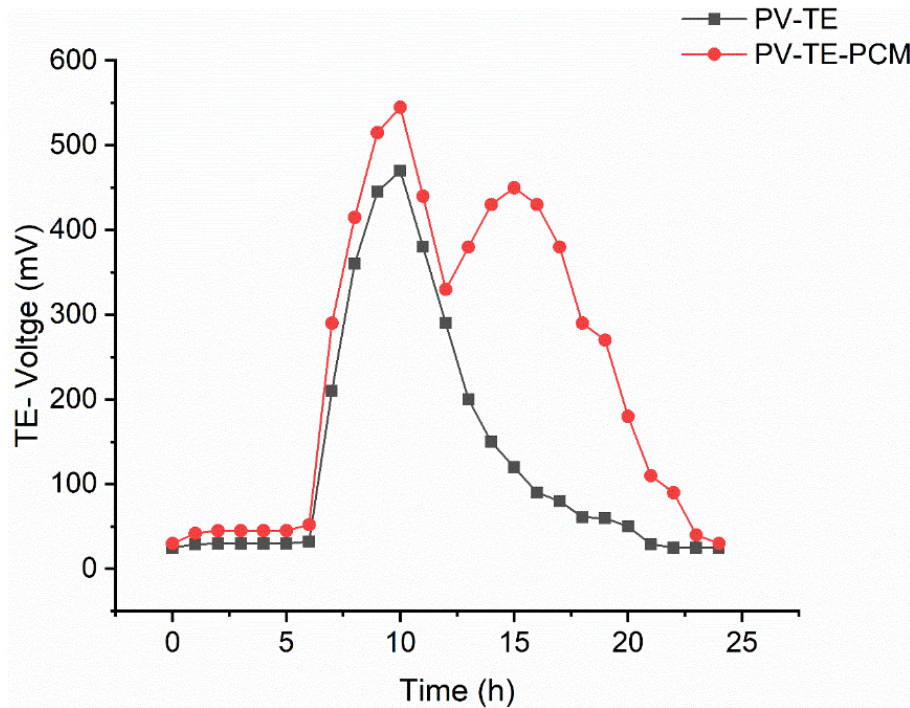


Figure (5.12) Electricity generation by TE device



Figure (5.13) Electricity generation at night

### 5-3-6 I-V and P-V Curves

This part of the results demonstrates the effect of reducing temperature of the module on the photovoltaic characteristics, which is the output of the study of solar panel current, voltage, power and efficiency obtained by the solar module analyzer system. The solar module analyzer produces the characteristic curve (I-V) and (I-P) curves by changing the internal resistive load from zero to infinity with time [47] . Voltage and current of the PV-TE and PV-PCM-TE modules are greater than PVREF. The highest intensity of solar radiation was recorded at 1:00 PM. Figures (5-15) and (5-16) show curves (I-V, P-V), respectively, where the PV-PCM-TE curve showed the best peak current as well as the best power because its temperature is lower than the rest of the curves.



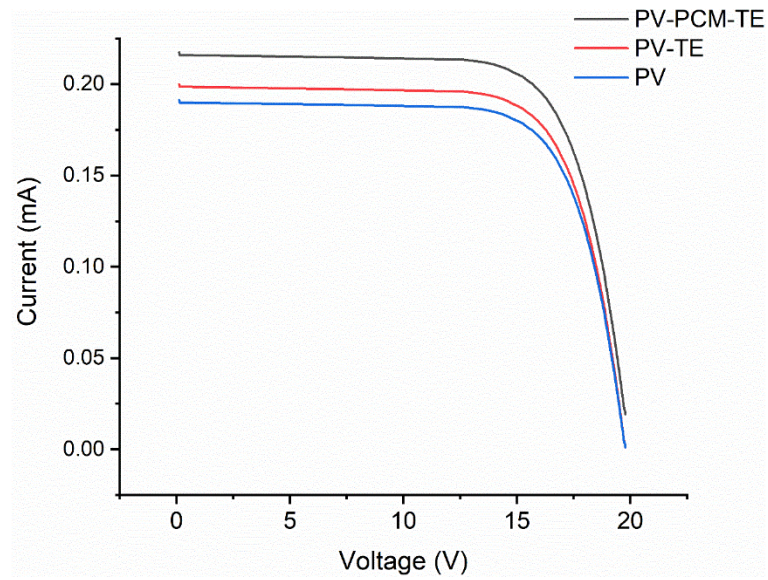


Figure (5.15) Comparison of the solar cell's Current-Voltage curves.

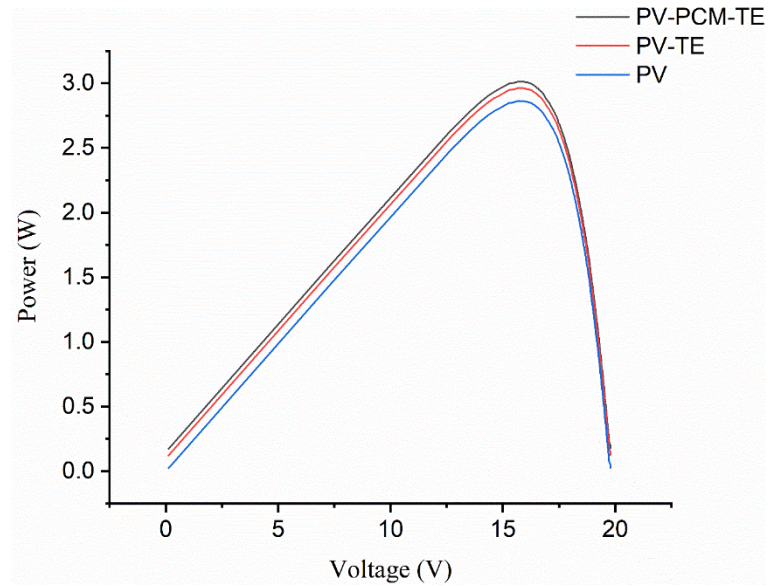


Figure (5.16) Comparison of the solar cell's Power-Voltage curves

### 5-5 Economic Feasibility

From the researcher's point of view The world cleanest energy source is solar energy, which also has a number of advantages and benefits. For instance, the energy from the sun provides the earth for one hour might provide all of the world's energy needs for a whole year. The most significant environmental issues for solar cells are high temperatures and reflection issues. Solar cells are subject to numerous environmental issues that have a negative impact on their efficiency. The addition of a phase changing material is an effective way to improve the performance of the cell, as the cell temperature decreases and the energy is stored for the purpose of using it at night for the purpose of generating electricity in Table (5-1) Economic analysis of the price of cells, phase changing material and TE device.

Table (5.1) materials Cost

<b>Materials</b>		<b>Unit</b>		<b>Unit Price</b>	
PV		1		14 USD	
TE device		1		3 USD	
PCM (SP-31)		1-gram		0.06 USD	
MODEL	Price of PV and TE	TE	PCM	Price	
PV	14 USD	-----	-----	14 USD	
PV-TE	32 USD	6 * (3 USD)	-----	32 USD	
PV-PCM-TE	32 USD	6 * (3 USD)	200 grams	44 USD	

## **CHAPTER SIX**

### **CONCLUSIONS AND RECOMMENDATIONS**

#### **6.1 Conclusion**

The current study investigates the effect of adding a phase changing material behind the solar cell for the purpose of improving the performance of polycrystalline silicon solar cells. All experiments were conducted in the city of Najaf, Iraq (44°20;23 N 32°01;44 E) for the month of May.

- 1- The addition of a phase-changing material is an effective way to improve the performance of polycrystalline solar cells by cooling the bottom of the cell.
- 2- The cell surface temperature was clearly reduced, as the maximum variation of 2.5 °C was obtained compared to the base cell, which led to an increase in the electrical energy produced and an increase in the efficiency of the cell.
- 3- The possibility of generating electricity from two models depending on a thermal electric device, where the rate of electricity generation during the day for the PV-TE model was 42 mV, while at night 6.8 mV, for the model of the PV- PCM-TE, the generation rate during the day was 65 mV and at night 10.2 mV
- 4- The maximum output power is (290 mW) with no PCM and (305 mW) is reported as PCM behind the photovoltaic panel.
- 5- The efficiency increases in the presence of the phase-changing material, where it reaches (14 %) at the peak.

## **6.2 Recommendations**

This study focused on PCM materials used to improve polycrystalline silicon solar cells, and to improve this work, some ideas should be included in future studies:

1. Applying different types of PCM (Phase Chang Material) materials, and studying their effect on the performance of solar cells.
2. Modifying the used model and use it in the opposite direction of the sun, where the exchanger is above and the solar cell is reversed downwards.
3. Studying the effect of the size of the solar cell and the size of devices (thermal electric device) on electricity generation.
4. Using new devices that extend the same principle (Thermal Electric device).



## REFERENCES

- [1] T. Zhang, M. Wang, and H. Yang, “A review of the energy performance and life-cycle assessment of building-integrated photovoltaic (BIPV) systems,” *Energies*, vol. 11, no. 11, 2018, doi: 10.3390/en11113157.
- [2] P. Moriarty and D. Honnery, “Energy efficiency or conservation for mitigating climate change?,” *Energies*, vol. 12, no. 18, pp. 1–17, 2019, doi: 10.3390/en12183543.
- [3] S. Ghasemian, A. Faridzad, P. Abbaszadeh, A. Taklif, A. Ghasemi, and R. Hafezi, “An overview of global energy scenarios by 2040: identifying the driving forces using cross-impact analysis method,” *Int. J. Environ. Sci. Technol.*, no. 0123456789, 2020, doi: 10.1007/s13762-020-02738-5.
- [4] A. M. Alsayah, M. H. K. Aboaltabooq, M. H. Majeed, and A. A. Al-Najafy, “Multiple modern methods for improving photovoltaic cell efficiency by cooling: A review,” *J. Mech. Eng. Res. Dev.*, vol. 42, no. 4, pp. 71–78, 2019, doi: 10.26480/jmerd.04.2019.71.78.
- [5] J. R. Lim, J. F. Whitacre, J. P. Fleurial, C. K. Huang, M. A. Ryan, and N. V. Myung, “Fabrication method for thermoelectric nanodevices,” *Adv. Mater.*, vol. 17, no. 12, pp. 1488–1492, 2005, doi: 10.1002/adma.200401189.
- [6] A. Proto *et al.*, “Thermal energy harvesting on the bodily surfaces of arms and legs through a wearable thermo-electric generator,” *Sensors (Switzerland)*, vol. 18, no. 6, 2018, doi: 10.3390/s18061927.

- [7] S. N. Gorbacheva, V. V. Makarova, and S. O. Ilyin, “Hydrophobic nanosilica-stabilized graphite particles for improving thermal conductivity of paraffin wax-based phase-change materials,” *J. Energy Storage*, vol. 36, no. February, p. 102417, 2021, doi: 10.1016/j.est.2021.102417.
- [8] S. Jamali, M. Yari, and S. M. S. Mahmoudi, “Enhanced power generation through cooling a semi-transparent PV power plant with a solar chimney,” *Energy Convers. Manag.*, vol. 175, no. July, pp. 227–235, 2018, doi: 10.1016/j.enconman.2018.09.004.
- [9] E. D. Rounis, A. K. Athienitis, and T. Stathopoulos, “Multiple-inlet Building Integrated Photovoltaic/Thermal system modelling under varying wind and temperature conditions,” *Sol. Energy*, vol. 139, no. 1, pp. 157–170, 2016, doi: 10.1016/j.solener.2016.09.023.
- [10] J. C. Mojumder, W. T. Chong, H. C. Ong, K. Y. Leong, and Abdullah-Al-Mamoon, “An experimental investigation on performance analysis of air type photovoltaic thermal collector system integrated with cooling fins design,” *Energy Build.*, vol. 130, pp. 272–285, 2016, doi: 10.1016/j.enbuild.2016.08.040.
- [11] R. Sellami and M. E. Slimani, “Study and modeling of energy performance of a hybrid photovoltaic / thermal solar collector : Configuration suitab,” *Energy Convers. Manag.*, vol. 125, pp. 209–221, 2016.
- [12] A. Fudholi *et al.*, “Energy and exergy analyses of photovoltaic thermal collector with  $\nabla$ -groove,” *Sol. Energy*, vol. 159, no. November 2016, pp. 742–750, 2018, doi:

10.1016/j.solener.2017.11.056.

- [13] S. Senthilraja, R. Gangadevi, R. Marimuthu, and M. Baskaran, “Performance evaluation of water and air based PVT solar collector for hydrogen production application,” *Int. J. Hydrogen Energy*, vol. 45, no. 13, pp. 7498–7507, 2020, doi: 10.1016/j.ijhydene.2019.02.223.
- [14] N. Xu, J. Ji, W. Sun, W. Huang, J. Li, and Z. Jin, “Numerical simulation and experimental validation of a high concentration photovoltaic/thermal module based on point-focus Fresnel lens,” *Appl. Energy*, vol. 168, pp. 269–281, 2016, doi: 10.1016/j.apenergy.2016.01.077.
- [15] M. Modjinou, J. Ji, J. Li, W. Yuan, and F. Zhou, “A numerical and experimental study of micro-channel heat pipe solar photovoltaics thermal system,” *Appl. Energy*, vol. 206, no. May, pp. 708–722, 2017, doi: 10.1016/j.apenergy.2017.08.221.
- [16] R. Liang, C. Zhou, Q. Pan, and J. Zhang, “Performance evaluation of sheet-and-tube hybrid photovoltaic/thermal (PVT) collectors connected in series,” *Procedia Eng.*, vol. 205, pp. 461–468, 2017, doi: 10.1016/j.proeng.2017.10.411.
- [17] A. L. Abdullah, S. Misha, N. Tamaldin, M. A. M. Rosli, and F. A. Sachit, “Theoretical study and indoor experimental validation of performance of the new photovoltaic thermal solar collector (PVT) based water system,” *Case Stud. Therm. Eng.*, vol. 18, no. November 2019, p. 100595, 2020, doi: 10.1016/j.csite.2020.100595.

- [18] T. Maatallah, R. Zachariah, and F. G. Al-Amri, “Exergo-economic analysis of a serpentine flow type water based photovoltaic thermal system with phase change material (PVT-PCM/water),” *Sol. Energy*, vol. 193, no. May, pp. 195–204, 2019, doi: 10.1016/j.solener.2019.09.063.
- [19] A. Naghdbishi, M. E. Yazdi, and G. Akbari, “Experimental investigation of the effect of multi-wall carbon nanotube – Water/glycol based nanofluids on a PVT system integrated with PCM-covered collector,” *Appl. Therm. Eng.*, vol. 178, 2020, doi: 10.1016/j.applthermaleng.2020.115556.
- [20] A. Kane and V. Verma, “Performance enhancement of building integrated photovoltaic module using thermoelectric cooling,” *Int. J. Renew. Energy Res.*, vol. 3, no. 2, pp. 320–324, 2013, doi: 10.20508/ijrer.81220.
- [21] J. Zhang, H. Zhai, Z. Wu, Y. Wang, and H. Xie, “Experimental investigation of novel integrated photovoltaic-thermoelectric hybrid devices with enhanced performance,” *Sol. Energy Mater. Sol. Cells*, vol. 215, no. April, p. 110666, 2020, doi: 10.1016/j.solmat.2020.110666.
- [22] T. Wang, S. Wang, and W. Wu, “Experimental study on effective thermal conductivity of microcapsules based phase change composites,” *Int. J. Heat Mass Transf.*, vol. 109, pp. 930–937, 2017, doi: 10.1016/j.ijheatmasstransfer.2017.02.068.
- [23] J. F. Luo *et al.*, “Numerical and experimental study on the heat transfer properties of the composite paraffin/expanded graphite phase

- change material,” *Int. J. Heat Mass Transf.*, vol. 84, pp. 237–244, 2015, doi: 10.1016/j.ijheatmasstransfer.2015.01.019.
- [24] P. Lv, C. Liu, and Z. Rao, “Experiment study on the thermal properties of paraffin/kaolin thermal energy storage form-stable phase change materials,” *Appl. Energy*, vol. 182, pp. 475–487, 2016, doi: 10.1016/j.apenergy.2016.08.147.
- [25] Q. Sun, Y. Yuan, H. Zhang, X. Cao, and L. Sun, “Thermal properties of polyethylene glycol/carbon microsphere composite as a novel phase change material,” *J. Therm. Anal. Calorim.*, vol. 130, no. 3, pp. 1741–1749, 2017, doi: 10.1007/s10973-017-6535-6.
- [26] W. Wu, W. Wu, and S. Wang, “Form-stable and thermally induced flexible composite phase change material for thermal energy storage and thermal management applications,” *Appl. Energy*, vol. 236, no. November 2018, pp. 10–21, 2019, doi: 10.1016/j.apenergy.2018.11.071.
- [27] C. Li, Q. Li, and Y. Ding, “Investigation on the thermal performance of a high temperature packed bed thermal energy storage system containing carbonate salt based composite phase change materials,” *Appl. Energy*, vol. 247, no. November 2018, pp. 374–388, 2019, doi: 10.1016/j.apenergy.2019.04.031.
- [28] R. N. Wijesena, N. D. Tissera, V. W. S. G. Rathnayaka, H. D. Rajapakse, R. M. de Silva, and K. M. N. de Silva, “Shape-stabilization of polyethylene glycol phase change materials with chitin nanofibers for applications in ‘smart’ windows,” *Carbohydr. Polym.*, vol. 237, p. 116132, 2020, doi: 10.1016/j.carbpol.2020.116132.

- [29] W. Q. Li, Z. G. Qu, Y. L. He, and Y. B. Tao, “Experimental study of a passive thermal management system for high-powered lithium ion batteries using porous metal foam saturated with phase change materials,” *J. Power Sources*, vol. 255, pp. 9–15, 2014, doi: 10.1016/j.jpowsour.2014.01.006.
- [30] Y. B. Tao, C. H. Lin, and Y. L. He, “Preparation and thermal properties characterization of carbonate salt/carbon nanomaterial composite phase change material,” *Energy Convers. Manag.*, vol. 97, pp. 103–110, 2015, doi: 10.1016/j.enconman.2015.03.051.
- [31] A. Hussain, C. Y. Tso, and C. Y. H. Chao, “Experimental investigation of a passive thermal management system for high-powered lithium ion batteries using nickel foam-paraffin composite,” *Energy*, vol. 115, pp. 209–218, 2016, doi: 10.1016/j.energy.2016.09.008.
- [32] A. C. Evers, M. A. Medina, and Y. Fang, “Evaluation of the thermal performance of frame walls enhanced with paraffin and hydrated salt phase change materials using a dynamic wall simulator,” *Build. Environ.*, vol. 45, no. 8, pp. 1762–1768, 2010, doi: 10.1016/j.buildenv.2010.02.002.
- [33] O. Beerli, O. Rotem, E. Hazan, E. A. Katz, A. Braun, and Y. Gelbstein, “Hybrid photovoltaic-thermoelectric system for concentrated solar energy conversion: Experimental realization and modeling,” *J. Appl. Phys.*, vol. 118, no. 11, 2015, doi: 10.1063/1.4931428.
- [34] A. Reznia, D. Sera, and L. A. Rosendahl, “Coupled thermal model of

- photovoltaic-thermoelectric hybrid panel for sample cities in Europe,” *Renew. Energy*, vol. 99, pp. 127–135, 2016, doi: 10.1016/j.renene.2016.06.045.
- [35] W. Zhu, Y. Deng, Y. Wang, S. Shen, and R. Gulfam, “High-performance photovoltaic-thermoelectric hybrid power generation system with optimized thermal management,” *Energy*, vol. 100, pp. 91–101, 2016, doi: 10.1016/j.energy.2016.01.055.
- [36] M. Benghanem, A. A. Al-Mashraqi, and K. O. Daffallah, “Performance of solar cells using thermoelectric module in hot sites,” *Renew. Energy*, vol. 89, pp. 51–59, 2016, doi: 10.1016/j.renene.2015.12.011.
- [37] D. Li, Y. Xuan, Q. Li, and H. Hong, “Exergy and energy analysis of photovoltaic-thermoelectric hybrid systems,” *Energy*, vol. 126, pp. 343–351, 2017, doi: 10.1016/j.energy.2017.03.042.
- [38] J. Zhang and Y. Xuan, “Performance improvement of a photovoltaic - Thermoelectric hybrid system subjecting to fluctuant solar radiation,” *Renew. Energy*, vol. 113, pp. 1551–1558, 2017, doi: 10.1016/j.renene.2017.07.003.
- [39] T. Cui, Y. Xuan, E. Yin, Q. Li, and D. Li, “Experimental investigation on potential of a concentrated photovoltaic-thermoelectric system with phase change materials,” *Energy*, vol. 122, pp. 94–102, 2017, doi: 10.1016/j.energy.2017.01.087.
- [40] R. Bjørk and K. K. Nielsen, “The maximum theoretical performance of unconcentrated solar photovoltaic and thermoelectric generator

- systems,” *Energy Convers. Manag.*, vol. 156, no. September 2017, pp. 264–268, 2018, doi: 10.1016/j.enconman.2017.11.009.
- [41] G. Li, X. Chen, and Y. Jin, “Analysis of the primary constraint conditions of an efficient photovoltaic-thermoelectric hybrid system,” *Energies*, vol. 10, no. 1, pp. 1–12, 2017, doi: 10.3390/en10010020.
- [42] Y. P. Zhou, M. J. Li, Y. H. Hu, and T. Ma, “Design and experimental investigation of a novel full solar spectrum utilization system,” *Appl. Energy*, vol. 260, no. November 2019, p. 114258, 2020, doi: 10.1016/j.apenergy.2019.114258.
- [43] H. G. Hameed, “Numerical and Experimental Study of Flow and Heat Transfer Enhancement in a Cylindrical Heat Pipe Using Nanofluid,” no. January, p. 278, 2015, doi: 10.13140/RG.2.2.20344.08960.
- [44] E. Gedik, “Experimental Investigation of Module Temperature Effect on Photovoltaic Panels Efficiency,” *J. Polytech.*, vol. 19, no. 4, pp. 569–576, 2016.
- [45] M. A. R. Sadiq Al-Baghdadi, Z. M. H. Noor, A. Zeiny, A. Burns, and D. Wen, “CFD analysis of a nanofluid-based microchannel heat sink,” *Therm. Sci. Eng. Prog.*, vol. 20, p. 100685, 2020, doi: 10.1016/j.tsep.2020.100685.
- [46] B. B. GARDAS and M. . TENDOLKAR, “Design of Cooling System for Photovoltaic Panel for Increasing Its Electrical Efficiency,” *Int. J. Mech. Ind. Eng.*, pp. 65–69, 2013, doi: 10.47893/ijmie.2013.1129.
- [47] A. Thesis, “Experimental and numerical study for enhancement of the performance of hybrid solar pv modules,” no. September, 2021.





# APPENDIX – A

## Data Sheet



### SP31



The creation of the latent heat material RUBITHERM® SP has led to a new and innovative class of low flammability PCM. RUBITHERM® SP consists of a unique composition of inorganic components. RUBITHERM® SP is preferably used as macroencapsulated material. Densities of more than 1,0 kg/l are achieved. This and all properties mentioned below make RUBITHERM® SP to the preferred PCM used in construction. Both passive and active cooling can easily be realized. We look forward to discussing your particular questions, needs and interests with you.

**Properties:**

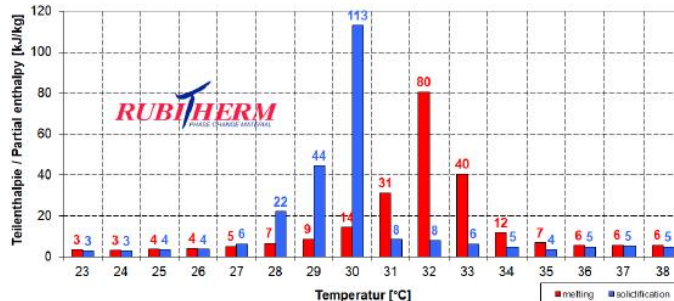
- stable performance throughout the phase change cycles
- high thermal storage capacity per volume
- limited supercooling (2-3K dependig on volume and cooling rate),
- low flammability, non toxic
- different melting temperatures between -50°C und 70°C are available
- encapsulation necessary, minimum volume: 50ml

#### The most important data:

	Typical Values	
<b>Melting area</b>	<b>31-33</b>	[°C]
	main peak: 32	
<b>Congealing area</b>	<b>28-30</b>	[°C]
	main peak: 30	
<b>Heat storage capacity ± 7,5%</b> Combination of sensible and latent heat in a temperatur range of 23 °C to 38 °C.	<b>210</b>	[kJ/kg]
<b>Specific heat capacity</b>	<b>58</b>	[Wh/kg]*
	<b>2</b>	[kJ/kg·K]*
<b>Density solid</b> at 15°C	<b>1,35</b>	[kg/l]
<b>Density liquid</b> at 35°C	<b>1,3</b>	[kg/l]
<b>Volume expansion</b>	<b>3-4</b>	[%]
<b>Heat conductivity</b>	<b>~0,5</b>	[W/(m·K)]
<b>Max. operation temperature</b>	<b>50</b>	[°C]
<b>Corrosion</b>	corrosive effect on metals	

*Note: The product must be initialized (melt, homogenize and cool to 0 °C) once before use to achieve the specified properties. Many SP-product are hygroscopic and may absorb moisture if stored improperly. This can result in a change of the physical properties given.*

Beispiel / example: SP31 Teilenthalpie / Partial enthalpy distribution\*



Rubitherm Technologies GmbH  
 Imhoffweg 6  
 D-12307 Berlin  
 phone: +49 (30) 7109622-0  
 E-Mail: info@rubitherm.com  
 Web: www.rubitherm.com

The product information given is a non-binding planning aid, subject to technical changes without notice. Version: 09.11.2020

## APPENDIX – B

### THERMOCOUPLE'S CALIBRATION

In this study, eight K-type thermocouples were used to measure the temperature distribution across the flat tube radiator pipe as well as the input and output fluid temperature. The calibration certificate by the manufacturer as shows in Figure A1. For optimum temperature reading, all the thermocouples were calibrated with an alcohol thermometer by using a water bath as shown in Figure A2.

<b>THERMOCOUPLES</b>	
<b>CERTIFICATE OF QUALITY</b>	
<b>PRODUCT</b>	TEHRMOCOUPLES
<b>MODE</b>	SNNT-02
<b>SPECIFICATION</b>	2M- $\frac{1}{4}$ "
<b>TYPE</b>	K
<b>MEASUREMENT RANGE</b>	0~800 °C
<b>INSPECTOR</b>	
<b>DATE</b>	
	<b>QC PASS</b>

Figure A1. The calibration certificate by the manufacturer for thermocouples



Figure A2. Thermocouple's calibrations and data logger

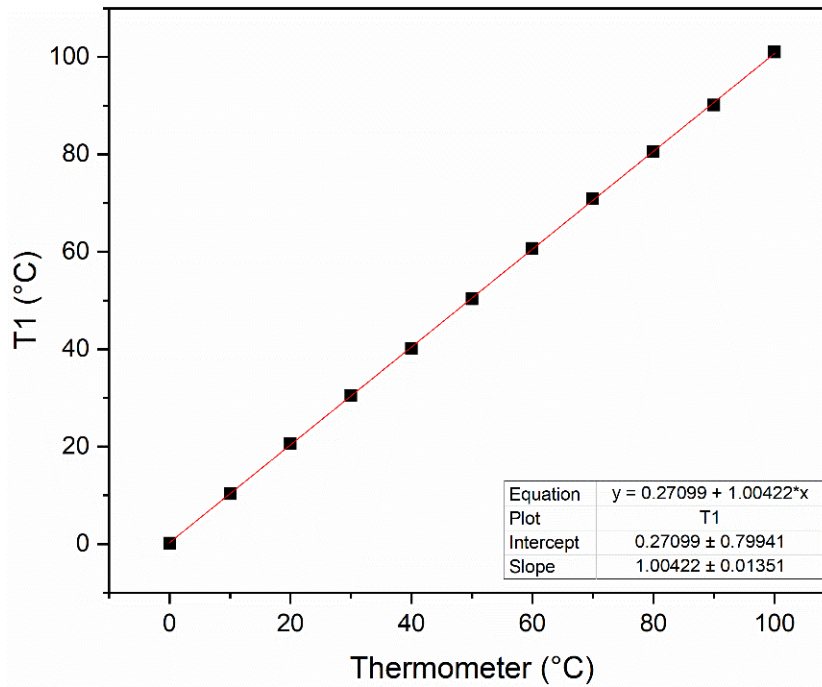


Figure A3. T1 thermocouples calibration

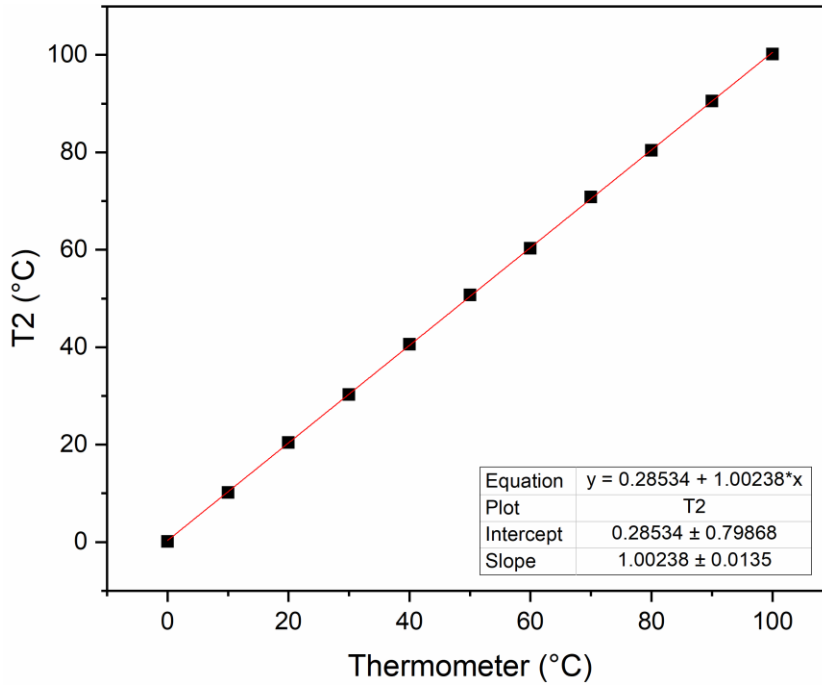


Figure A4. T2 thermocouples calibration

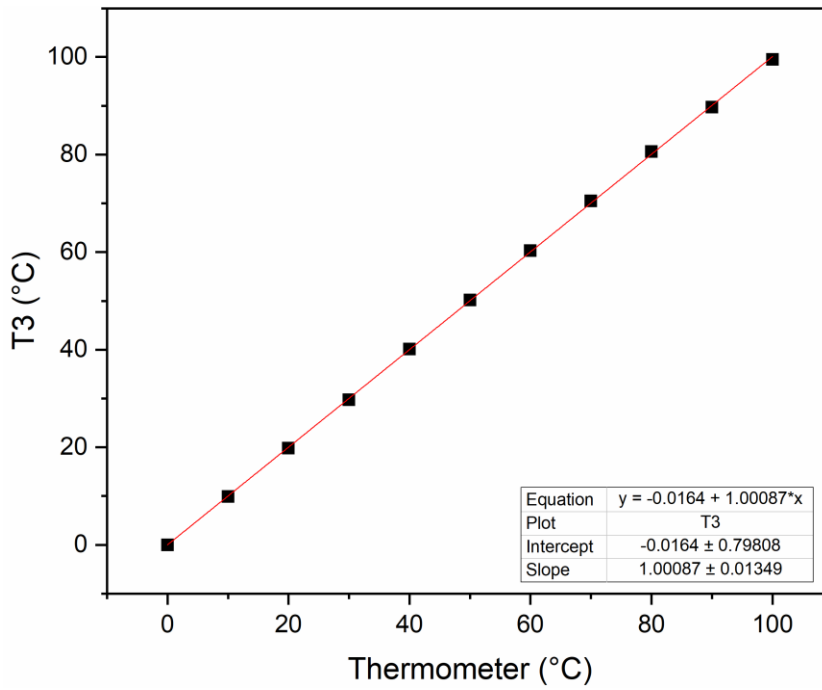


Figure A5. T3 thermocouples calibration

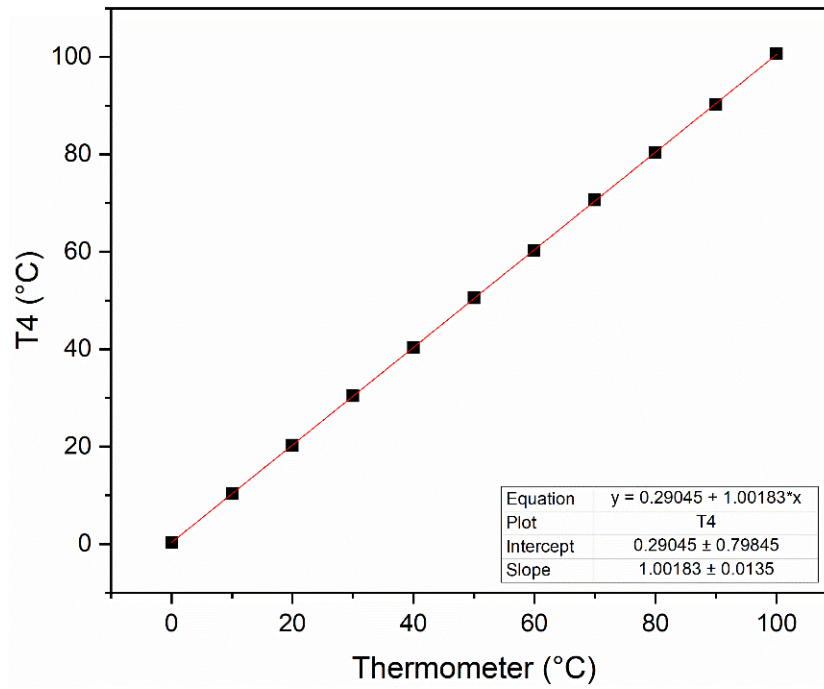


Figure A6. T4 thermocouples calibration

## APPENDIX - C

### WIND SPEED CALIBRATION

In this study, an AM-4206M anemometer was used to measure wind speed. It was calibrated with the Davis standard weather station installed above the ground in the Technical College of Engineering in Najaf / Iraq. Figure B1 shows the results of the calibration.

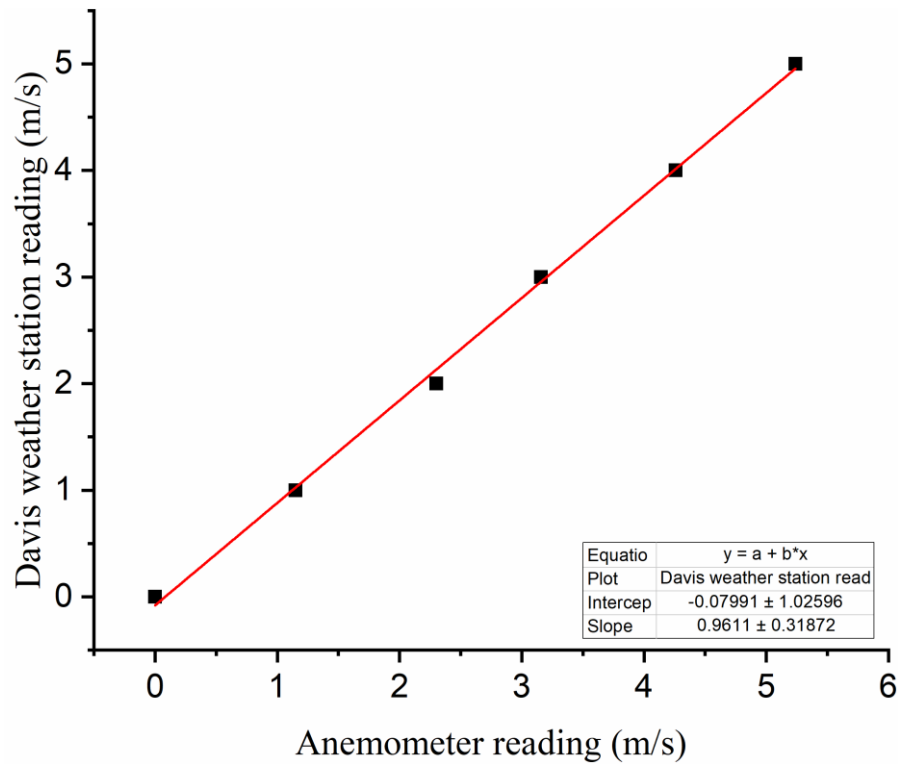


Figure B1 Anemometer Calibration

**Appendix-D.**  
**Solar Meter Calibration:**

Figure and table c.1. Represent the calibration process for the solar meter (Pyranometer) device which was used in this work. Figure C1 solar meter calibration (Pyranometer)

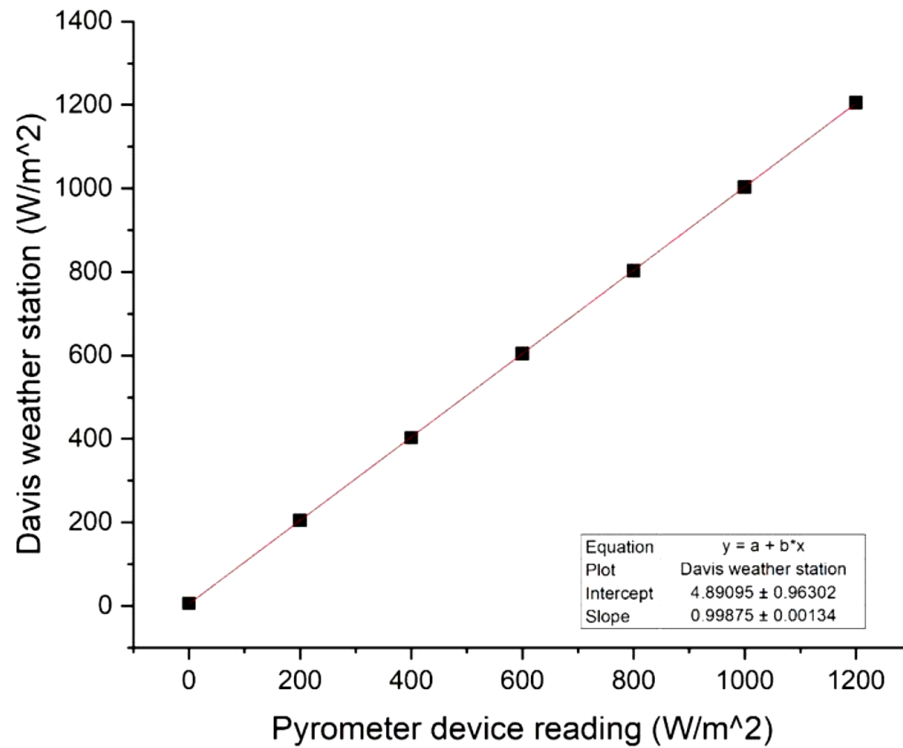


Figure C1 solar meter calibration (Pyranometer)



# Appendix-E

## LIST OF PUBLICATIONS

### Paper 1

HARBIN GONGYE DAXUE XUEBAO/JOURNAL OF HARBIN INSTITUTE OF TECHNOLOGY



#### ACCEPTANCE LETTER TO AUTHOR

Manuscript ID: HIT-2022-10851

DATE: 01-08-2022

Dear Authors,

**Ammar Al-Daamee<sup>\*1</sup>, Ali najah Al-Shamani<sup>2</sup> & Karaar Mahdi Al-Araji<sup>3</sup>**

*\*1,2 Department of Technical Power Mechanics, Technical Engineering College / Najaf, Iraq  
3 Al-Furat Al-Awsat Technical University, (ATU), Najaf, Iraq*

With reference to your paper submitted “Generating electricity at night based on a hybrid solar cell” we are pleased to accept the same for publication in the upcoming issue of **Journal of Harbin Institute of Technology**.

Your quick cooperation in editing the manuscript and completing it appropriately with the reviewers' opinion will work on publishing your article as soon as possible.

I believe that our collaboration will help to accelerate the global knowledge creation and sharing one step further. Please do not hesitate to contact me if you have any further questions.

We thank you for considering our journal as a venue to publish your research work.

Sincerely,

**Editorial Office**

<http://hebgydxxb.periodicals.com/index.php/JHIT>

<https://www.scopus.com/sourceid/29708>

Publisher: Harbin Gongye Daxue/Harbin Institute of Technology

ISSN: 0367-6234

Harbin Gongye Daxue  
Xuebao/Journal of Harbin...

Q3

Engineering  
(miscellaneous)

best quartile

SJR 2021

0.21

powered by scimagojr.com

**GENERATING ELECTRICITY AT NIGHT BASED ON A HYBRID SOLAR CELL****Ammar Al-Daamee<sup>\*1</sup>, Ali Najah Al-Shamani<sup>2</sup> & Karaar Mahdi Al-Araji<sup>3</sup>**<sup>\*1,2&3</sup>Department of Technical Power Mechanics, Technical Engineering College / Najaf, Al-Furat Al-Awsat Technical University, (ATU), Najaf, Iraq**ABSTRACT**

Photovoltaic thermal conversion (PV-TE) is one of the important ways to generate electrical energy by converting solar energy into electrical energy by relying on the Seebeck effect of the thermoelectric device (TE) on the basis of the waste heat of solar cells. By attaching the TE device to the bottom of the solar cell with a heat sink on the other side of the TE The voltage of the TE device was measured for the first models (PV-TE) and the second (PV-PCM-TE) and its value was (10.2,6.8) mV at night respectively, which means that electricity can be generated both day and night, and it can be used for many applications such as small screens and sensors.

**Keywords:** Electrical, Renewable energy, Thermal, Night, PV-TE.

DOI:[10.11720/JHIT.54082022.27](https://doi.org/10.11720/JHIT.54082022.27)

**1. INTRODUCTION**

Fossil fuels and nonrenewable sources are in high demand for current energy, yet they are also major greenhouse gas emitters. The use of renewable energy sources is one of the solutions to the present energy difficulties. Solar energy is a renewable energy source that is both clean and infinite resource that produces no waste and emits no carbon dioxide There have been studies conducted to have benefited from vast solar resources over time Photovoltaic panels (PV) are one of the most essential technologies, but their efficiency is low since much of the solar energy is converted into electricity. converting thermal energy [1] Photovoltaic cells (PV) are solar-powered devices that convert incoming sunlight into direct current electricity. During the energy conversion process, these cells only convert a fraction of the incoming solar radiation into useable output energy, with the remainder being wasted as heat. As a result, the temperature of the cell rises due to this lost heat. The open-circuit voltage and fill factor fall as the temperature of the photovoltaic cell rises, lowering the PV system's conversion efficiency [2] . Researchers rely on the emissivity of the sky because solar radiation



# Using Hybrid System Photovoltaic Thermal /Phase Change Materials / Thermoelectric (PVT/PCM/TE): A Review

<sup>1\*</sup>Ammar Maythem, <sup>2</sup>Ali Najah Al-Shamani

<sup>1,2</sup>Department of Technical Power Mechanics, Technical Engineering College / Najaf, Al-Furat Al-Awsat Technical University  
(ATU), Najaf, Iraq

\*corresponding contact: ammar.faisal.ms.etcn @student.atu.edu.iq

## Abstract

During the last few decades, PV/T technology has attracted a large number of researchers and experts. In this research, previous research on Photovoltaic thermal (PVT), phase-changing material (PCM) and thermoelectric (TE) are collected for the purpose of knowing the properties and efficiency of each part so that we can collect them in one system and study their efficiency and the factors that affect them for the purpose of studying the possibility of generating electricity at night.

**Keywords:** Electrical, Renewable energy, Thermal, night, PV-TE.

---

## 1-1 INTRODUCTION

The depletion of conventional fossil fuel supplies has reignited interest in the use of renewable energy resources. As a result, an alternative energy source must be determined in order to meet our energy needs while also preserving conventional fossil resources. Solar energy is a renewable form of energy that has the potential to meet a considerable portion of the world's energy consumption. The evolution of renewable energy sources [1], such as solar energy, has resulted in a source of energy that is both environmentally friendly and clean. Solar energy is also a viable solution for the impoverished and rural populations who are unable to access contemporary energy sources. Solar energy can be used to generate both thermal and electrical energy. These two energies are produced in different ways, but if hybrid collectors are utilized, they can be produced simultaneously. The photovoltaic-thermal (PVT) collector is a hybrid system that combines two types of collectors: thermal and solar. A PVT collector is a device that collects solar energy, converts it to thermal and electrical energy, and then transfers the thermal energy to the fluid flowing into the collector [2]. PV panel, insulation, and frame make up a PVT collector. As a result, a PVT collector is made up of one or more covers

## Paper 3



### 1<sup>st</sup> International Conference on Achieving the Sustainable Development Goals

(6<sup>th</sup> – 7<sup>th</sup>) June 2022 in Istanbul- Turkey

## Initial Acceptance Letter

**Manuscript Number: 132**

**Dear:** Ammar Al-Daamee

**Co-Authors:** Ali najah Al-Shamani, Dhafer Manea Hachim, Karaar Mahdi Al-Araji

**Congratulations!**

It is a great pleasure to inform you that, following the peer review process, your manuscript titled

**(Numerical study of the sustainable energy generated from a photovoltaic panel with the addition of a phase change material)**

had been **ACCEPTED** for participating in the **1<sup>st</sup> International Conference on Achieving the Sustainable Development Goals**, and is being considered for publication in **(AIP Conference proceeding)**.

Thank you for your significant contribution to the ICASDG2022 conference.

A handwritten signature in green ink, appearing to be 'Ahmed G. Wadday', written over a light blue horizontal line.

**Prof. Dr. Ahmed G. Wadday**

**ICASDG2022 Scientific Committee Chair | AIP Conference Proceeding Editor**

**6<sup>th</sup> – 7<sup>th</sup> June 2022 | Istanbul | Turkey**

## الخلاصة

على مدار القرن الماضي ، كانت العديد من مجالات البحث الأساسية والتطبيقية مدفوعة بالرغبة في إنتاج الطاقة من الموارد المتجددة. يعد استخدام الخلايا الكهروضوئية ، التي تُعرف أحيانًا باسم الكهروضوئية ، طريقة مباشرة ومتطورة لالتقاط الطاقة الشمسية التي تعتبر أحد أفضل الخيارات للطاقة المتجددة بدون ضوضاء أو تلوث أو أجزاء متحركة ، فالأجهزة الكهروضوئية (الخلايا الشمسية) غير معتادة في أنها تحول الطاقة الشمسية العارضة مباشرة إلى كهرباء ، مما يجعلها قوية ويمكن الاعتماد عليها وطويلة الأمد. تعد كفاءة تحويل الطاقة المنخفضة للخلايا الكهروضوئية ، والتي تؤدي إلى مزيد من الفشل خلال وقت التشغيل عن طريق رفع درجة حرارة الخلية فوق حد معين ، أحد أهم التحديات في استخدام الأنظمة الشمسية. غالبًا ما يتم تقليل الكفاءة الكهربية للوحدات الكهروضوئية بنسبة 35٪ بسبب إشعاع الشمس المنعكس عن اللوحة.

أجريت الدراسة في الكلية التقنية بالنجف ، فوق سقوف مبنى قسم تقنيات الهندسة الميكانيكية للطاقة ، النجف / العراق خلال شهر أيار عام 2022 ، من حيث تأثير (تغير العوامل والظروف الجوية ، كتلة PCM).

خلال هذه الدراسة ، تم التحقق من فائدة إضافة مادة متغيرة الطور تحت الخلايا الشمسية لغرض التبريد والاستفادة من الطاقة المخزنة أثناء الليل ، وبالتالي زيادة كفاءتها وزيادة الطاقة الناتجة. كانت الدراسة في جزئين ، عملي وعددي ، تم من خلالها اختبار ثلاثة نماذج ( PV ، PV-TE ، PV-PCM-TE). عدديًا ، تم اختبار مادة تغيير الطور لعدة أنواع ( SP-31 ، SP-50 ، SP-58 ، SP-70 ، SP-90 ) ، حيث كان SP-31 هو أفضل أداء حراري. بناءً على الاختبارات العملية التي تم إجراؤها لمدة 24 ساعة في شهر مايو للوحدات الثلاث ، كانت السعة الناتجة من PV ، PV-TE ، PV-PCM-TE ( 365 ، 369 ، 375 ) ملي واط. تم تسجيل كفاءة ( 14.58 ، 14.65 ، 14.14٪ ) على التوالي. كانت الكهرباء التي تم توليدها من PV-TE و PV-PCM-TE خلال النهار 62.42 ملي فولت وبمعدل 10.1 و 6.8 ملي فولت في الليل على التوالي ، ويمكن استخدام هذه الطاقة التي تم توليدها في الليل من أجل أجهزة استشعار وشاشات دقيقة وبعض التطبيقات الأخرى.



دراسة عملية وعددية لزيادة كفاءة النظام الحراري الضوئي باستخدام مادة متغيرة الطور

رساله مقدمه الى

قسم هندسه تقنيات ميكانيك القوى كجزء من متطلبات نيل درجه ماجستير تقني في هندسة  
الحراريات

تقدم بها

عمار ميثم فيصل مذبوب

اشراف

د. علي نجاح كاظم

أب 2022